Pergamon

J Mech Phys Solids, Vol 43, No. 1, pp 49–90, 1995

0022-5096/95 $9 50+0 00

0022-5096(94)00056-5

MECHANICS OF THE HYDROGEN–DISLOCATION–IMPURITY INTERACTIONS—I. INCREASING SHEAR MODULUS

P. SOFRONIS† and H. K. BIRNBAUM‡

†Department of Theoretical and Applied Mechanics, and ‡Department of Materials Science and Engineering, University of Illinois at Urbana-Champaign, IL, U.S A

(*Received* 20 *October* 1993; *in revised form* 13 *August* 1994)

ABSTRACT

The effect of hydrogen on dislocation–dislocation and dislocation–impurity atom interactions is studied under conditions where hydrogen is in equilibrium with local stresses and in systems where hydrogen increases the shear modulus. In the case of two edge dislocations (plane strain) the effect of hydrogen is modeled by a continuous distribution of dilatation lines whose strength depends on the local hydrogen concentration. The hydrogen distribution in the atmospheres is adjusted to minimize the energy of the system as the dislocations approach each other. The iterative finite element analysis used to calculate the hydrogen distribution accounts for the stress relaxation associated with the hydrogen induced volume and the elastic moduli changes due to hydrogen. The interactions between the dislocations are calculated accounting for all the stress fields due to dislocations and hydrogen atmospheres. Modeling of the hydrogen effects on the edge dislocation–interstitial solute atom interaction and on the screw dislocation–interstitial solute atom interaction is discussed using a finite element analysis and the atom interaction energies are calculated in the presence of hydrogen. For the case where hydrogen increases the shear modulus, a significant hydrogen-related decrease of the edge dislocation–interstitial solute atom interaction energy was observed when the edge dislocation–solute distance is approximately less than two Burgers vectors. Depending on the orientation of the tetragonal axis of the interstitial solute distortion field, hydrogen may strengthen or weaken the interaction between the screw dislocation–interstitial solute.

1. INTRODUCTION

Direct observations of the effects of hydrogen on dislocations under stress (Tabata and Birnbaum, 1984; Robertson and Birnbaum, 1986; Bond *et al.*, 1987, 1988; Rozenak *et al.*, 1990; Shih *et al.*, 1988) have shown that the velocities of edge, screw and mixed dislocations are increased by the presence of hydrogen in solid solution in FCC, BCC and HCP crystal structures, and in relatively pure metals and alloys. The generality of the effect suggests it derives from the elastic interactions between dislocations and barriers to their motion. Hydrogen-enhanced dislocation velocity under stress is the physical basis of the hydrogen-enhanced localized plasticity (HELP) model of hydrogen embrittlement (Sirois *et al.*, 1992; Sirois and Birnbaum, 1992). Hydrogen "shielding" of the elastic interactions between dislocations and short range stress fields has been suggested as the mechanism responsible for HELP (Birnbaum and Sofronis, 1994). The underlying principle of the hydrogen shielding mechanism

is that hydrogen diminishes the local stress fields from dislocations and solutes which act as barriers to the dislocation motion.

The effects of solute atoms on the behavior of dislocations, and their equilibrium distribution at a dislocation, have been studied by Cottrell (1948), Cottrell and Jawson (1949), Cottrell and Bilby (1949), Bilby (1950), and Hirth and Lothe (1982). According to Cottrell (1948), the first order elastic interaction energy (Eshelby, 1957) associated with a hydrogen atom introduced against the stress field, σ_{ij}^a, of a defect is given by

$$W_{\text{int}}^{(1)} = -\tfrac{1}{3}\sigma_{kk}^a \Delta v' = -\tfrac{1}{3}\sigma_{kk}^a \Delta v, \tag{1}$$

where $\Delta v'$ is the unconstrained volume dilatation and denotes the difference in volume of the hydrogen atom before its introduction into the lattice and that of the interstitial lattice space available to host the hydrogen atom, and $\Delta v = \Delta v'$ is the volume change of the host metal lattice per hydrogen atom (Hirth and Lothe, 1982). In this paper, Cartesian tensors and vectors are denoted by bold-face roman letters ($\mathbf{A}, \mathbf{a}$) and their scalar components by the corresponding light-face italic letters (A_{ij}, a_i). Indices are understood generally to range over 1, 2 and 3 and the repeated index summation convention is used. The volume change, Δv, is directly related to the partial molar volume of hydrogen, $V_{\text{H}} = \Delta v N_{\text{A}}$ where N_{A} is Avogadro's number. It is assumed in (1) that the solution is dilute and the hydrogen-induced strains are approximately purely dilatational.

In addition to the first order elastic interaction, which arises from the volume change associated with the solute atom, there is a second order elastic interaction (Eshelby, 1955, 1956; Hirth and Lothe, 1982), which arises from the additional change in the potential energy resulting from the change of the moduli upon the introduction of the stress center (solute atom) in the lattice while the external loads, σ_{ij}^a, are held fixed. This second order elastic interaction can be written as

$$W_{\text{int}}^{(2)} = \tfrac{1}{2}(C'_{ijkl} - C_{ijkl})\varepsilon'_{ij}\varepsilon^a_{kl} v_{\text{s}}, \tag{2}$$

where v_{s} is the volume over which the solute atoms alter the elastic stiffnesses, C_{ijkl}, the strains ε_{ij}^a are those caused by the external stress, σ_{ij}^a, in the absence of the solute atom, and strains ε'_{ij} are the elastic strains inside the volume v_{s} after the solute atom has been introduced in the lattice in the presence of the external stresses σ_{ij}^a which are held constant. The primed stiffnesses correspond to those characteristic of the local stiffnesses in the presence of the solute atom, and the value of v_{s} is usually taken as the volume of the solute atom. In general, the second order interaction energy is much smaller than the first order interaction energy. In the vicinity of a dislocation, the second order interaction energy decreases with distance from the dislocation as $1/r^2$, in contrast to the $1/r$ dependence of the first order interaction energy. In the case of an isotropic solid, the second order elastic interaction is manifest primarily through the dependence of the shear modulus and bulk modulus on the solute concentration. While the first order interaction dominates the solute interactions with edge dislocations, the dominant interaction term for screw dislocations is the second order interaction for those solutes having isotropic distortion fields (e.g. H interstitials),

and the first order interaction for solutes having distortion fields with symmetries lower than cubic (e.g. C interstitials).

In this paper the micromechanics of the shielding mechanism is investigated from a continuum mechanics viewpoint and illustrative calculations are carried out for a few important cases. The material is considered linearly elastic, isotropic, and local constitutive moduli changes due to hydrogen are allowed for. Neglect of elastic anisotropy, chosen to simplify the calculations, will have a number of consequences which should be explored at a later time as the effects *may* have some significance. The presence of elastic anisotropy can introduce dilatational fields for screw dislocations and alter the elastic field of the H solutes. In the present paper the calculations are carried out for the case where the shear modulus *increases* with the addition of hydrogen to solid solution. In a subsequent paper the calculations will be presented for the case where hydrogen *decreases* the shear modulus of the solid. Hydrogen concentrations in the stress fields of microstructural defects are studied under steady state, equilibrium conditions. The Fermi–Dirac form (Hirth and Carnahan, 1978) is used to calculate the equilibrium hydrogen concentration C, measured in atoms of hydrogen per unit lattice volume, under stress in terms of the remote unstressed lattice concentration C_0 as

$$C = \frac{C_0}{\dfrac{C_0}{\beta N_L} + \left(1 - \dfrac{C_0}{\beta N_L}\right)\exp\left(\dfrac{W_{int}}{kT}\right)}, \tag{3}$$

where β denotes the number of interstitial sites per solvent atom, N_L denotes the number of solvent lattice atoms per unit lattice volume, k is Boltzmann's constant, T is the absolute temperature and W_{int} is the interaction energy. For the numerical calculations, the H/M ratio was taken as a maximum of 1 corresponding to $\beta = 6$ and $\theta = 1/6$ for the tetrahedral interstitial site occupancy typical of BCC systems. The mechanical effect of hydrogen is modeled through the stress field of a continuous distribution of dilatation centers in space, with the strength of a center taken proportional to the local hydrogen concentration. Transient effects or solute drag on moving dislocations of the type calculated by Fuentes-Samaniego *et al.* (1984) are not accounted for.

In discussing the interaction of hydrogen with dislocations the significant effect of hydrogen on the moduli (Mazzolai and Birnbaum, 1985a, b) should be taken into account. This is particularly significant for the hydrogen–screw dislocation interaction as the first order interaction energy is zero, since hydrogen has a spherical distortion field (Peisl, 1978), while the second order interaction energy is nonzero. In the case where hydrogen increases the shear modulus, the case discussed in the present paper, the second order interaction energy with the screw dislocation is positive and hence it decreases the local hydrogen concentration around the screw dislocation. Since these calculations are carried out for the low hydrogen concentration case, the effects on the hydrogen concentration at the screw dislocation are small and may be neglected. In a subsequent publication the results will be presented for the case where hydrogen decreases the shear modulus.

A description of the hydrogen effect on the interaction between two edge dis-

locations is presented in Section 2.1 with a treatment in which the elastic moduli are treated as unaffected by hydrogen. The stress fields of the hydrogen atmospheres which vary pointwise are integrated to estimate the hydrogen effect on the interaction between the dislocations. Stress relaxation and modulus change effects (for the case of the *increase* of the shear modulus with solute hydrogen) on the interaction between two edge dislocations are assessed in Section 2.2 with an iterative finite element analysis. The same finite element methodology is used to study the hydrogen effect on the interaction between an interstitial impurity atom (C) with (a) an edge dislocation in Section 3.1, and (b) a screw dislocation in Section 3.2.

2. HYDROGEN EFFECT ON THE INTERACTION BETWEEN TWO EDGE DISLOCATIONS

2.1. *Analytical calculation*

In the absence of hydrogen, the interaction force per unit length between two parallel dislocations is given (Hirth and Lothe, 1982) by

$$\mathbf{F} = \boldsymbol{\sigma}_1 \mathbf{b}_2 \times \boldsymbol{\xi}, \tag{4}$$

where $\boldsymbol{\sigma}_1$ is the stress tensor of dislocation 1, $\mathbf{b}_i$, $i = 1,2$, are the Burgers vectors, and $\boldsymbol{\xi}$ is the unit vector along the dislocation lines. In the case to be discussed, parallel edge dislocations, (4) results in a repulsive force if the dislocations are of the same sign and on the same slip system. In this case, the force on dislocation 2 due to dislocation 1 is $\tau_D b_2$, where τ_D is the stress of dislocation 1 resolved along the slip plane and Burgers vector.

The hydrogen effect on the interaction between the dislocations 1 and 2 is assessed by calculating the hydrogen-induced change to the shear stress τ_D due to interactions between the hydrogen atmospheres surrounding the two dislocations. These hydrogen atmospheres are modeled by a continuous distribution of dilatation lines parallel to the dislocation lines each acting as a stress source which affects the shear stress, τ_D. This model is consistent with the plane strain assumption for the dislocation strain field when the hydrogen concentration does not vary in the direction of the dislocation lines. The in-plane concentration of the dilatation lines, n, is directly related to the hydrogen concentration per unit volume, C, through

$$n = Ch, \tag{5}$$

where h is the distance between two successive hydrogen atoms along the dilatation line and the concentration n denotes the number of hydrogen atoms per unit area in the plane normal to the dilatation line. In the following subsections hydrogen effects on the constitutive moduli are neglected. They are discussed in a later section.

2.1.1. *The stress field of a single hydrogen dilatation line.* The line of dilatation associated with hydrogen atoms introduced into a stress-free lattice is produced in a continuum sense by replacing a cylindrical hole of infinite length and radius r_0 in an infinite lattice with a cylinder of the same material and radius $r_0 + \varepsilon r_0$, where ε is a small positive number related to the volume of solution of hydrogen. Relative to a

polar cylindrical coordinate system r, ϕ and x_3, where the x_3 axis coincides with the dilatation line, one may write the nonzero stress components of the plane strain axisymmetric field, σ_{ij}, at a distance r from the dilatation line as

$$\sigma_{rr} = -\frac{\mu \Delta a}{\pi r^2}, \quad \sigma_{\phi\phi} = \frac{\mu \Delta a}{\pi r^2}, \tag{6}$$

where

$$\Delta a = \frac{\Delta a'}{2(1-\nu)} \tag{7}$$

denotes the strength of the dilatation line, and $\Delta a' = 2\pi r_0 \varepsilon$ is the "unconstrained area of expansion". Due to combined axial symmetry and plane strain, only the displacement, u, in the r direction in the x_3 plane is nonzero and is given by

$$u = \frac{\Delta a}{2\pi r}. \tag{8}$$

The strain field associated with u is incompressible and the area flux in the x_3 plane through a circular boundary enclosing the dilatation line is $\Delta A = \Delta a$. The unconstrained area of expansion, $\Delta a'$, can be evaluated in terms of the unconstrained volume change, $\Delta v'$, of a hydrogen atom. Consistent with the plane strain assumption of the model, the unconstrained volume of the unit length cylinder, $\Delta a'$, used to produce the dilatation line is equal to the total unconstrained volume $\Delta v'/h$ of the $1/h$ hydrogen atoms which make the unit length of the cylinder. Therefore, $\Delta a' = \Delta v'/h$. In view of the fact that $\Delta v = \Delta v'$, one may write $\Delta a' = \Delta v/h$. Since the volume change, Δv, is related to the partial molar volume of hydrogen in solution, V_H,

$$\Delta a' = \frac{V_H}{N_A h}. \tag{9}$$

2.1.2. *Interaction of a single dilatation line with an applied stress.* Assume that a dilatation line is introduced in an infinite elastic solid subject to stresses, σ^a_{ij}, with corresponding displacements, u^a_i, caused by externally applied loads. Using (6)–(8), one finds the interaction energy per unit length between the stress field, σ_{ij}, of the dilatation line and the stress field, σ^a_{ij}, due to the external loads as (Eshelby, 1956)

$$E_{int} = \oint_s (\sigma_{ij} u^a_i - \sigma^a_{ij} u_i) n_j \, ds = -\frac{\sigma^a_{11} + \sigma^a_{22}}{2} \Delta a', \tag{10}$$

where s is any arbitrary curve on the x_3 plane encircling the dilatation line, stress components σ^a_{ij} are measured in a Cartesian coordinate system whose axis, x_3, coincides with the hydrogen dilatation line, and $\mathbf{n}$ is the outward unit normal vector to the curve. In (10), which is the plane version of (1), dividing E_{int} by the total number of hydrogen atoms, $1/h$, in the unit length of the dilatation line, one finds the interaction energy per hydrogen atom as $W_{int} = E_{int} h$. Therefore, with use of (9) and (10), one obtains W_{int} as

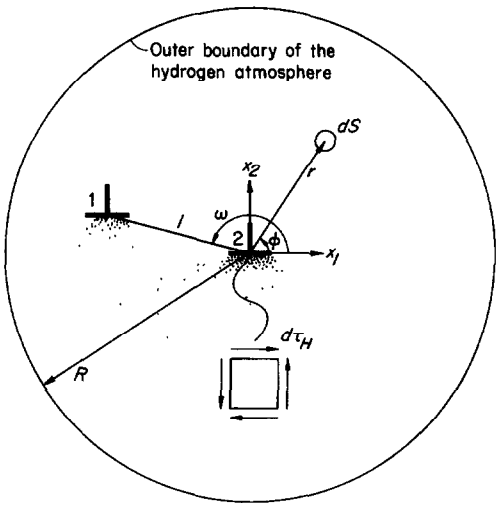

Fig. 1. Schematic model indicating the shear stress $d\tau_H$ induced at the core of the dislocation 2 by the hydrogen dilatation lines of an infinitesimal area dS at position (r, ϕ). The radius R of the hydrogen atmosphere stretches as far as infinity.

$$W_{int} = -\frac{\sigma^a_{11}+\sigma^a_{22}}{2}\frac{V_H}{N_A}. \tag{11}$$

Equation (11) is used in (3) to calculate the hydrogen concentration C in equilibrium with an applied stress field, σ^a_{ij}, and (5) provides the density n of the dilatation lines in the plane normal to the dislocation lines. Since the stress field, σ^a_{ij}, varies with position, so also do the fields C and n.

2.1.3. *Integrated shear stress effect of the hydrogen dilatation lines on a dislocation.* Consider a Cartesian coordinate system of axes x_1 and x_2 centered at the core of the dislocation 2, as shown in Fig. 1, and a single hydrogen dilatation line at a point with polar coordinates r and ϕ. The shear stress exerted at the core of dislocation 2 along the slip plane by the hydrogen dilatation line can be found from (6) as

$$\frac{\sigma_{rr}-\sigma_{\phi\phi}}{\pi r^2}\sin 2\phi = -\frac{\mu\Delta a}{\pi r^2}\sin 2\phi. \tag{12}$$

Using the principle of linear superposition and (12), one may calculate the shear stress, $d\tau_H$, due to the dilatation lines of an infinitesimal area, dS, at r, ϕ (see Fig. 1) as

$$d\tau_H = n\,dS\left(-\frac{\mu\Delta a}{\pi r^2}\right)\sin 2\phi. \tag{13}$$

Substituting (5), (7) and (9) into (13) and then integrating (13) over the entire area S occupied by the atmosphere, one finds the net shear stress, τ_H, induced by the hydrogen atmosphere as

$$\tau_H = -\frac{\mu}{2\pi(1-\nu)}\frac{V_H}{N_A}\int_0^{2\pi}\int_{r_2}^{R} C(r,\phi)\frac{\sin 2\phi}{r}\,dr\,d\phi, \tag{14}$$

where r_2 is the inner cut-off radius of dislocation 2 and R is the outer cut-off radius of the atmosphere centered at dislocation 2. The core of dislocation 1 with cut-off radius r_1 is also excluded from the integration. A similar expression can be written for the resolved shear stress on dislocation 1 due to hydrogen.

According to (6), the stress field of a hydrogen dilatation line is purely deviatoric. Consequently, the interaction energy, as calculated from (11), between the hydrogen dilatation lines is zero, i.e. the introduction of a dilatation line into the lattice is energetically independent of the presence of the neighboring lines. Therefore, the hydrogen concentration $C(r,\phi)$ at any position (r,ϕ) is determined solely by the corresponding stress due to dislocations 1 and 2. Superposition of the singular linear elastic stress fields of the two dislocations (Hirth and Lothe, 1982) yields the in-plane hydrostatic stress as

$$\frac{\sigma_{11}^a+\sigma_{22}^a}{2} = -\frac{\mu}{2\pi(1-\nu)}\left(b_2\frac{\sin\phi}{r}+b_1\frac{r\sin\phi - l\sin\omega}{r^2+l^2-2rl\cos(\phi-\omega)}\right), \tag{15}$$

where l and ω are the polar coordinates of the position of dislocation 1 (see Fig. 1). Then, concentration $C(r,\phi)$ in (14) is calculated by combining (3), (11) and (15).

Equations (6) indicate that the stress field of a hydrogen dilatation line decays as $1/r^2$ with distance, r. It is expected that the magnitude of the shear stress, τ_H, due to hydrogen on dislocation 2 will depend mainly on the dilatation lines close to the core of dislocation 2 and less on those which are remote from the core. This effect is seen in the integrand of (14), which diminishes as r increases and becomes zero at $r = \infty$, where $C(r,\phi) = C_0$. In the calculations for the hydrogen distribution and stresses on the dislocation, for fixed relative dislocation positions, (l,ω), the integral of (14) is computed numerically for an arithmetic progression of outer cut-off radii, R, differing by $20b_2$. The calculation is regarded as convergent when the relative error in the calculated shear stress for two successive radii is less than 10^{-3}. The details of the numerical integration are given in Appendix A.

Lastly, the corresponding shear stress, τ_D, resolved along the slip plane at the core of dislocation 2 due to dislocation 1 is given by

$$\tau_D = -\frac{\mu b_1}{2\pi(1-\nu)}\frac{\cos\omega\cos 2\omega}{l}. \tag{16}$$

The net shear stress exerted on dislocation 2 is equal to $\tau_D+\tau_H$.

2.1.4. *Numerical integration results.* All parameters, mechanical and hydrogen related, were chosen for the BCC niobium system whose lattice parameter is $a = 3.301$ Å with a corresponding Burgers vector magnitude, $b = 0.285\ 10^{-9}$ m. The elastic behavior of the niobium was assumed to be isotropic with a shear modulus of 30.8 GPa and a Poisson's ratio of 0.415, values which correspond to the hydrogen-free material. Given the ratio of volume expansion per hydrogen atom to volume of the host lattice atom is 0.174 (Peisl, 1975), one can calculate the partial molar volume

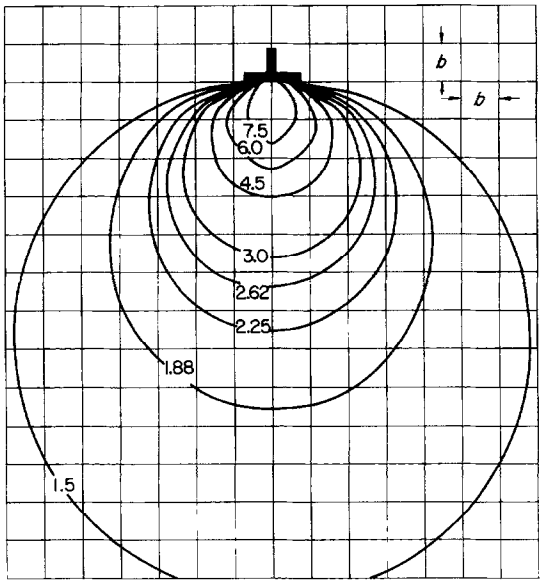

Fig. 2. Contours of normalized hydrogen concentration c/c_0 around a single edge dislocation at a nominal hydrogen concentration $c_0 = 0.1$ and temperature 300 K.

of hydrogen as $V_H = 0.188 \times 10^{-5}$ m^3 mol^{-1}. The molar volume of the metal was $V_M = 0.108 \times 10^{-4}$ m^3 mol^{-1}, which corresponds to $N_L = 0.555 \times 10^{29}$ solvent lattice atoms per m^3 of host metal lattice. The parameter β was chosen equal to six interstitial lattice atoms per solvent atom corresponding to tetrahedral site occupancy, thus allowing for local hydrogen concentrations capable of forming the NbH structure at $\theta = 1/6$. The system's temperature was 300 K.

The hydrogen atmosphere in equilibrium with the stress field of a single dislocation in an infinite medium is shown in the form of normalized iso-concentration lines, c/c_0, in Fig. 2 at a nominal concentration $c_0 = 0.1$ hydrogen atoms per solvent atom. The atmosphere is symmetric with respect to the dislocation plane because of the corresponding symmetry in the hydrostatic stress field of the dislocation. Under the same temperature and nominal hydrogen concentration, Figs 3 and 4 show the hydrogen atmosphere for dislocations 1 and 2 on the same slip system and at respective relative positions of 10, 8 and 6 Burgers vectors apart. In Fig. 4, the Burgers vector of dislocation 2 is negative. The hydrogen atmosphere around each dislocation is nonsymmetric when compared with the atmosphere of the single dislocation shown in Fig. 2. This is a direct result of the linear superposition in the stress field of the two dislocations. For dislocations of the same sign, the hydrostatic stress field is reinforced positively below the slip plane and negatively above the slip plane. For any given point in the area between the dislocations, this reinforcement increases as the dislocations approach each other. Consequently, the hydrogen concentration increases in the regions of positive stress enhancement and its value becomes larger than the concentration of the corresponding region in the atmosphere of a single dislocation. In contrast, the positive hydrostatic stress field of each dislocation is weakened in the case of dislocations of opposite sign and the hydrogen concentration in the tensile

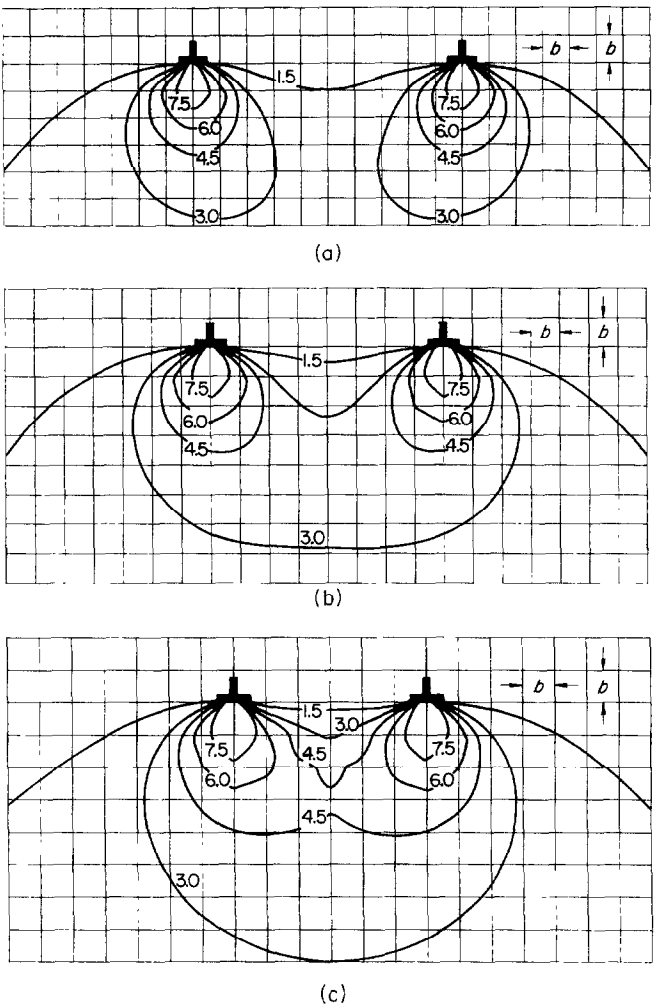

Fig. 3. Contours of normalized hydrogen concentration c/c_0 around two parallel edge dislocations of equal Burgers vectors with magnitude b and on the same slip system at a nominal hydrogen concentration $c_0 = 0.1$, temperature 300 K and dislocation distances (a) $10b$, (b) $8b$; (c) $6b$

regions of the two dislocations is less than that of a single dislocation alone. Figures 3(a)–(c) and 4(a)–(c) indicate that as the dislocations come closer, the iso-concentration curves become increasingly unsymmetrical.

In Figs 5 and 6, the hydrogen-induced shear stress, τ_H, resolved on the slip plane and along the Burgers vector at the core of dislocation 2, is plotted against distance, l, between the dislocations for nominal concentrations equal to 0.1, 0.01 and 0.001 hydrogen atoms per solvent atom, a temperature of 300 K and at an angle ω equal to 180° (see Fig. 1). In Fig. 6, dislocation 2 has a negative Burgers vector. The shear stress is normalized by the shear modulus μ and the distance by the Burgers vector magnitude, b. In the same figures the normalized shear stress, τ_D/μ, due to dislocation 1 in the absence of hydrogen, equation (16), and the total normalized shear stress,

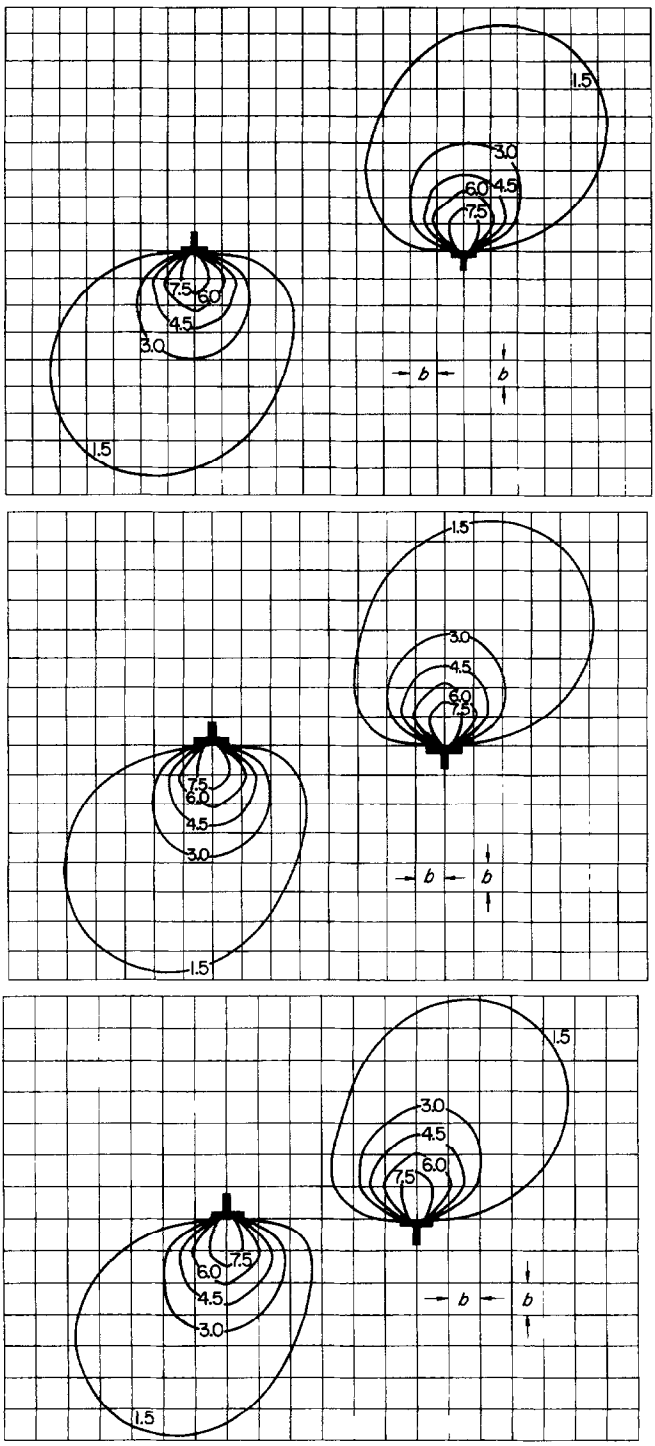

Fig. 4. Contours of normalized hydrogen concentration c/c_0 around two parallel edge dislocations of opposite and equal Burgers vectors with magnitude b and on the same slip system at a nominal hydrogen concentration $c_0 = 0.1$, temperature 300 K and dislocation distances: (a) $10b$; (b) $8b$; (c) $6b$.

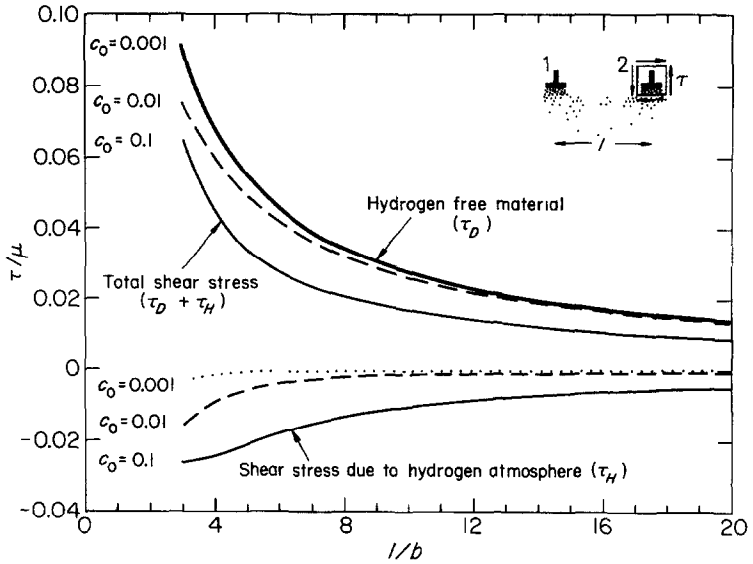

Fig. 5. Plot of the normalized shear stress, τ_H/μ, due to hydrogen, τ_D/μ, due to dislocation 1, and net shear stress, $(\tau_D+\tau_H)/\mu$, at the core of dislocation 2 along the slip plane versus normalized distance, l/b, at temperature 300 K and nominal hydrogen concentrations of H/M = 0.1, 0 01 and 0.001. The dislocation Burgers vectors were of the same sign.

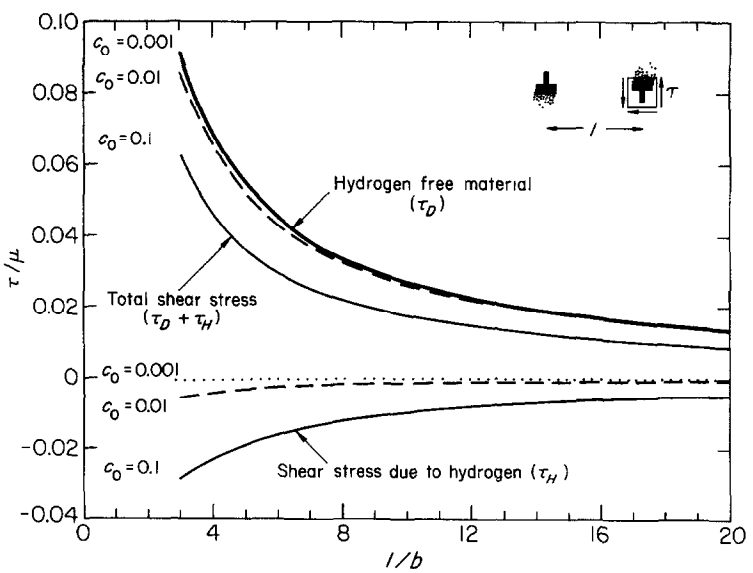

Fig. 6. Plot of the normalized shear stress, τ_H/μ, due to hydrogen, τ_D/μ, due to dislocation 1, and net shear stress, $(\tau_D+\tau_H)/\mu$, at the core of dislocation 2 along the slip plane versus normalized distance, l/b, at temperature 300 K and nominal hydrogen concentrations of H/M = 0.1, 0 01 and 0.001 The Burgers vector of dislocation 2 was negative.

$(\tau_D+\tau_H)/\mu$, are also plotted. Results for $l/b < 3$ were not calculated because they correspond to dislocation positions with very close or overlapping core regions.

The shear stress due to hydrogen is negative and its absolute value increases as the nominal concentration becomes larger, consistent with concentration dependence of the hydrogen dilatation line density, n, on C_0. The sign of the hydrogen-induced shear stress may be understood by examining the sign of the function $f(r, \phi) = -C(r, \phi)\sin(2\phi)/r$ in the integrand of (14). In both cases, the effect of hydrogen is to decrease the force exerted on dislocation 2 by dislocation 1.

2.2. *Finite element calculation*

In the preceding section it was assumed that the nature of each source of stress was unaffected by the presence of the others, i.e. that each dilatation line and dislocation produced stresses in the surrounding medium which were combined by the principle of linear superposition. The strength, and therefore the stress field, of each dilatation line was computed directly from the local hydrogen concentration as determined by the standard dislocation stress fields, thus allowing an analytic solution. However, the region close to dislocation can become saturated with solute atoms when the dilatation caused by the solutes equals that of the dislocation (Cottrell, 1948). This effect was not implicit in the treatment of the preceding section because of the approximation made, when expanding the lattice, that the consequent change in the forces exerted by the stress field on the dilating lattice may be neglected. According to Cottrell (1948) and Bilby (1950), this approximation is reasonable for a single solute atom but cannot be extended to the case where several solute atoms gather in the same region, since their contributions to the relaxation of the hydrostatic stresses are additive, leading to a saturation of the solute atmosphere.

In this section, the relaxed elastic stress field associated with the introduction of hydrogen into the lattice is calculated and the elastic moduli of the lattice are allowed to vary pointwise according to the local hydrogen concentration. Relaxation of the standard singular dislocation elastic stress field is not accounted for, even though it may be substantial in the region close to the core. Hydrogen from regions further afield is incapable of relaxing the dislocation singular stress field because the stresses due to hydrogen decay rapidly, as $1/r^2$. The total stress field in the lattice is found by superposition of the relaxed elastic stress due to hydrogen and that of the standard singular elastic dislocation stress field (Hirth and Lothe, 1982). The latter is calculated at a given position by using elastic moduli modified accordingly to the corresponding local hydrogen concentration. The hydrogen constitutive effect on the dislocation stress field is modeled by perturbing the modulus in the standard elastic solution for the hydrogen-free material.

2.2.1. *Hydrogen-induced transformation strain.* At a dilute local hydrogen concentration, $c = n_H/n_M$, where n_H moles of hydrogen are introduced into n_M moles of the solvent, the local unconstrained volume dilatation of the lattice volume, $V = n_M V_M$, is $\Delta V = n_H N_A \Delta v'$ and the corresponding unconstrained dilatational strain is $e^H = c\Delta v'/\Omega$, where Ω is the mean atomic volume of the host metal atom. Using the condition $\Delta v' = \Delta v$, one finds

$$e^{H} = c\frac{\Delta v}{\Omega}. \tag{17}$$

For a dilute solution, the concentration C which denotes hydrogen atoms per unit lattice volume is related to concentration c by

$$C = c\frac{N_A}{V_M} = \frac{c}{\Omega} = cN_L. \tag{18}$$

2.2.2. *Hydrogen effect on the elastic moduli of niobium.* High frequency acoustic measurements (Mazzolai and Birnbaum, 1985a, b) of the elastic constants C', C_{11} and C_L of the Nb–H(D) system were used to calculate the cubic moduli C_{11}, C_{12} and C_{44}. Over a wide range of hydrogen concentrations, the Nb–H system is elastically anisotropic with $C_{44} \neq (C_{11}-C_{12})/2$. This set of data allows the calculation of the Reuss and Voigt averages of the isotropic elastic moduli and these will be used in the calculations presented in a subsequent paper. In the present paper, the model material was assumed to be isotropic with bulk modulus, $B = (C_{11}+2C_{12})/3$, and shear modulus, $\mu = C_{44}$, which models the behavior in systems in which hydrogen increases the shear modulus. Using this procedure, and the data from Mazzolai and Birnbaum (1985a, b), the hydrogen effects on Young's modulus E, Poisson's ratio, ν, and shear modulus, μ, are described by

$$E = E_0(1+0.34c), \quad \nu = \nu_0 - 0.025c, \quad \mu = \mu_0\frac{1+0.34c}{1-0.0177c}, \tag{19}$$

where $E_0 = 87.1$ GPa, $\nu_0 = 0.415$ and $\mu_0 = 30.8$ GPa are Young's modulus, Poisson's ratio and shear modulus respectively for the hydrogen-free material. As will be seen, the conclusions about the hydrogen effect on the mechanical behavior of the material are strongly associated with the *assumed* increase of the shear modulus with increasing hydrogen concentration (which follows from the assumption $\mu = C_{44}$).

2.2.3. *Formulation of the boundary value problem for the hydrogen stress field.* Consider the hydrogen atmosphere associated with two parallel edge dislocations at a distance l apart on the same slip plane and of equal Burgers vector magnitude, b. Since hydrogen remote from the core of the dislocations is not expected to affect their interaction, modeling is confined to a finite square region, S, of the atmosphere centered at the midpoint between the dislocations (see Fig. 7). The outer boundary of the area S is placed within the remote region of the atmosphere where the hydrogen equilibrium concentration is essentially equal to C_0. In order to ensure that the hydrogen composition immediately inside S is exactly the same as that outside S, one has to apply image tractions along the outer boundary which arise mainly from the hydrogen close to the remote boundary since the hydrogen dilatation center stress field decays as $1/r^2$. Consequently, the contribution of the image tractions to the hydrogen equilibrium concentration close to the dislocation cores may be neglected in comparison to the effect of the singular hydrostatic stresses due to dislocations. Therefore, in the case of a dilute solution, those tractions can approximately be set equal to zero. The Fermi–Dirac form of (3) dictates that the region at and very close to the core is saturated with a finite amount of hydrogen and consequently no interior

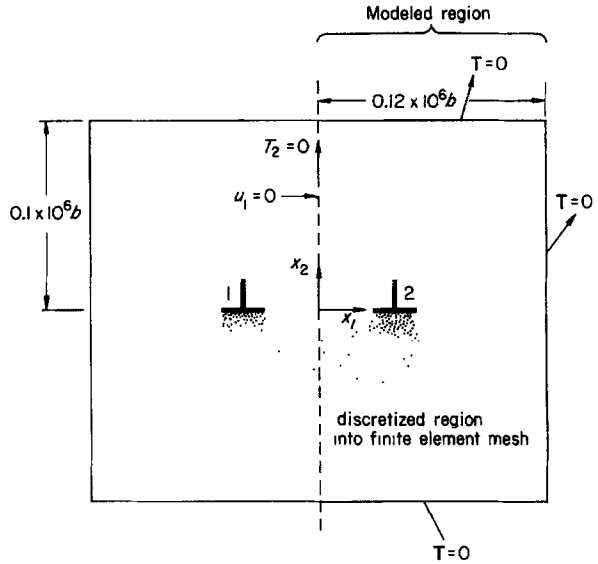

Fig. 7. Summary of the boundary value problem for the calculation of the hydrogen stress field. The superposed stress fields of dislocations 1 and 2 are used in the calculation of the hydrogen concentration which determines the transformation strain due to hydrogen and the elastic moduli throughout the modeled region.

holes corresponding to the dislocation cores were excluded from the area S, which remains simply connected.

The mechanical effect of hydrogen is modeled by a dilatational transformation strain whose components are given by

$$\varepsilon_{ij}^{H} = \tfrac{1}{3} e^{H} \delta_{ij}, \tag{20}$$

where δ_{ij} is the Kronecker delta. Transformation strain ε_{ij}^{H} varies pointwise and its magnitude depends upon the local hydrogen concentration as dictated by (17). The linear elasticity of the hydrogen–metal system accounting for transformation strain is characterized by

$$\sigma_{ij} = C_{ijkl}(\varepsilon_{ij} - \varepsilon_{ij}^{T}), \tag{21}$$

where σ_{ij} are the components of the elastic stress tensor due to hydrogen, ε_{ij} are the components of the net strain tensor which obey compatibility, $\varepsilon_{ij}^{T} = \varepsilon_{ij}^{H}$, and C_{ijkl} are the linear elastic moduli of the system, which are functions of position as dictated by (19) through the hydrogen concentration field. The mechanical equilibrium of the system in the absence of body forces is stated in the form of the principle of virtual work by

$$\int_{V} \sigma_{ij} \delta \varepsilon_{ij} \, \mathrm{d}V = 0, \tag{22}$$

where δ indicates an arbitrary virtual variation of the quantity it precedes, and V

denotes the volume of the rectangular domain S whose outer boundary is traction free.

The local hydrogen concentration is obtained from (3) with the interaction energy W_{int} furnished by (1), where σ_{ij}^a is the net hydrostatic stress due to all stress sources in the lattice. This procedure ignores the small effect of the second order elastic interaction on the calculation of the hydrogen concentration. Solution of hydrogen into the lattice requires that work be done against both the singular dislocation hydrostatic stress and the relaxed hydrostatic stress of the neighboring solutes. The former is unknown because the local moduli are concentration dependent. Thus, the hydrogen concentration as calculated through (1) and (3) is locally a nonlinear function of the unknown total hydrostatic stress. This implies that the local hydrogen composition needed to characterize the transformation strain in (20) and the local elastic moduli in (21), and required to solve the governing equations (21) and (22), can only be determined after the solution is found. Therefore, the problem of calculating the stress fields of the dislocation, the stress field due to hydrogen and the local distribution of hydrogen is coupled in a nonlinear sense and the solution procedure involves iteration. Assuming a solution for the hydrogen concentration field, one determines the transformation strain and the local constitutive moduli pointwise. Next, the resulting linear problem arising from (21) and (22) is solved and the solution for the hydrostatic stress is used to recalculate the hydrogen concentration through (1) and (3). The new solution for the concentration field is compared with the assumed one and the process continues until convergence is achieved. The hydrogen concentration in equilibrium with the hydrostatic stress found by superposition of the singular elastic fields of dislocations 1 and 2 can be used to initiate the process.

2.2.4. *Results.* An iterative finite element method was used to solve the boundary value problem (Sofronis and Birnbaum, 1993). First, a series of calculations was carried out by gradually moving the outer boundary of the rectangular region modeled further from the dislocations. The size of the region of integration used was sufficiently large so no dependence of the hydrogen distribution on the boundary position was observed. As a first approximation, (3) was used to calculate the hydrogen concentration in equilibrium with the superposed hydrostatic stress fields of the two edge dislocations at temperature 300 K and nominal concentration of $H/M = 0.1$. The interaction energy was found through (1) with all three components of the normal stress included in the calculation of the hydrostatic stress. No hydrogen effects on stress relaxation and the elastic moduli were considered and therefore no iterations were needed. The resulting hydrogen atmosphere shown in Fig. 8 may be compared with that of Fig. 3(c), which is also unrelaxed and calculated using only the two in-plane stress components [see (10)]. The iso-concentration lines in Fig. 8 are closer to the dislocations than the corresponding ones of Fig. 3(c), indicating that the hydrostatic stress at any given position is lower in the calculation when all three components are considered than in the case of the in-plane components, with the ratio of the two being $2(1+\nu)/3$.

At the next approximation, the effect of the volumetric transformation strain that accompanies the introduction of hydrogen into the lattice on stress relaxation (volumetric effect) was calculated by solving the relevant boundary value problem

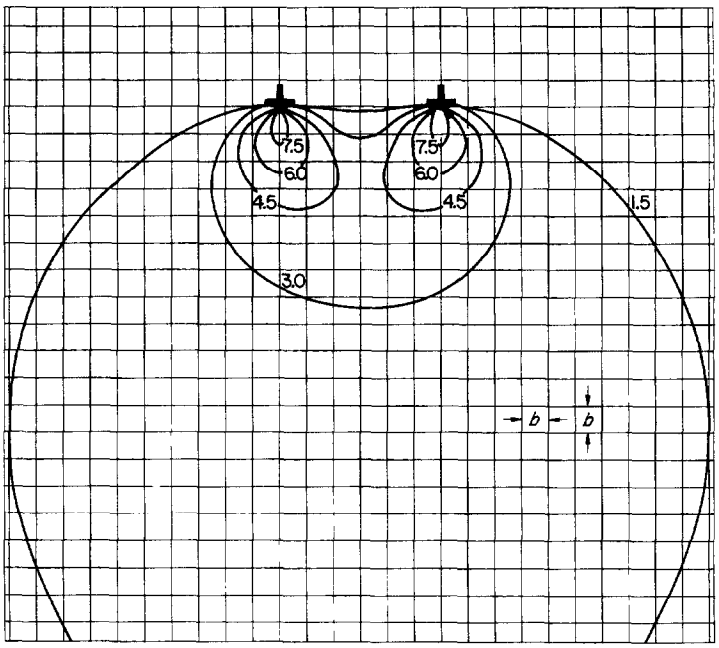

Fig. 8. Contours of the normalized hydrogen concentration c/c_0 around two parallel edge dislocations of equal Burgers vectors magnitude b and on the same slip system at a nominal hydrogen concentration $c_0 = 0.1$, temperature 300 K and distance $6b$. Hydrogen-induced relaxation of the hydrostatic stress and modulus change were not accounted for.

through iteration using the hydrogen-independent shear modulus, $\mu_0 = 30.8$ GPa, and Poisson's ratio, $\nu_0 = 0.415$, to allow examination of only the volumetric effect. The hydrogen atmosphere associated with the two edge dislocations at a distance of six Burgers vectors apart, and with the same parameters as used for the calculations shown in Figs 3 and 8, is shown in Fig. 9. The volumetric effect decreases the local hydrogen concentration, as can be seen by the iso-concentration contours, indicating that the volumetric effect relaxes the 3-D hydrostatic stress. Therefore, it is expected that the hydrogen-induced shear stress, τ_H, as estimated by the analytical calculation of the previous section and shown in Fig. 5 for various nominal concentrations, is greater in magnitude than the shear stress associated with the relaxed atmospheres furnished by the finite element calculations (Fig. 10), as seen by comparing Figs 5 and 10.

Next, the hydrogen volumetric effect was combined with the hydrogen-induced modulus change (modulus effect), as given by (19) using the iterative computation. The resulting hydrogen atmosphere at H/M = 0.1, 300 K and dislocation separation of $6b$ is shown in Fig. 11. Comparing Figs 11 and 10, one sees that the presence of both the volumetric and modulus effects increases the local concentration somewhat over those characteristic of the volumetric effect alone. Both of these concentrations are significantly less than those of the unrelaxed solution (Fig. 8). The differences in concentration for the different approximations reflect the differences in the local stresses. The increased concentration due to the modulus effect reflects the monotonic

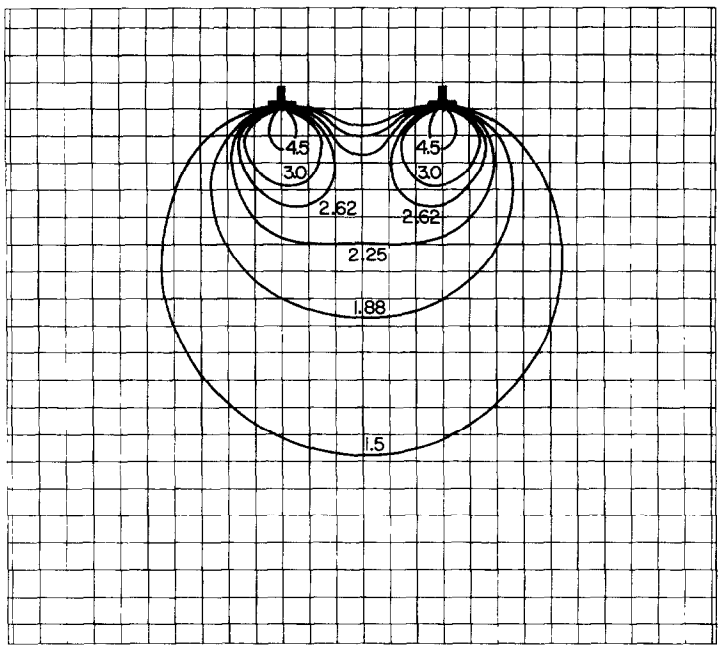

Fig. 9. Effect of the hydrogen-induced relaxation of the hydrostatic stress on the normalized hydrogen concentration c/c_0 around two parallel edge dislocations of equal Burgers vectors magnitude b and on the same slip system at a nominal hydrogen concentration $c_0 = 0.1$, temperature 300 K and distance $6b$. The hydrogen effect on the elastic moduli was not accounted for.

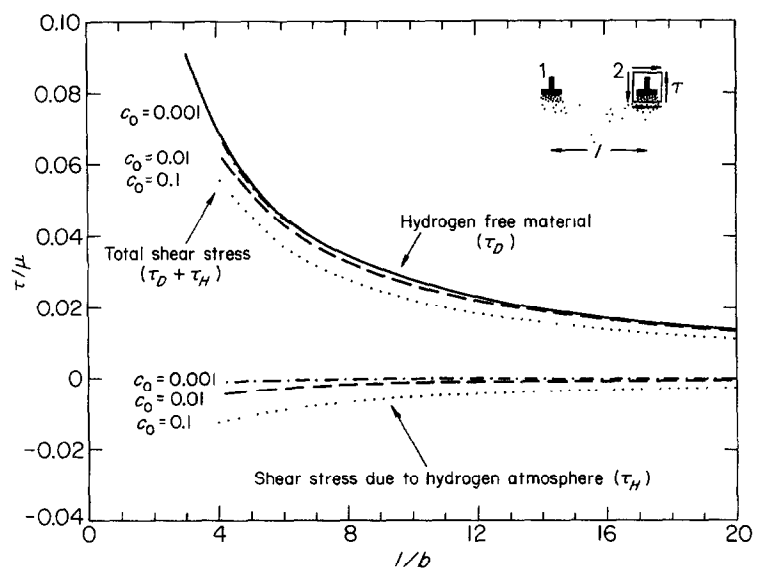

Fig 10. Effect of the hydrogen-induced relaxation of the hydrostatic stress on the normalized shear stress, τ_H/μ, due to hydrogen plotted versus dislocation distance, l/b, at temperature 300 K and nominal hydrogen concentrations of H/M = 0.1, 0.01 and 0.001. Stress τ_D/μ due to dislocation 1 and the net shear stress $(\tau_D+\tau_H)/\mu$ are also shown. The hydrogen effect on the elastic moduli was not accounted for

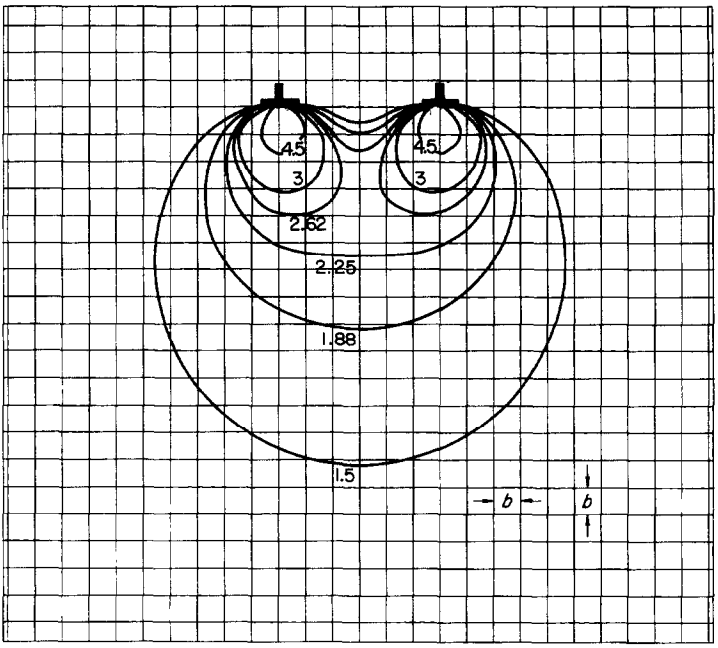

Fig. 11. Effect of the hydrogen-induced modulus change and relaxation of the hydrostatic stress on the normalized hydrogen concentration c/c_0 around two parallel edge dislocations of equal Burgers vectors magnitude b and on the same slip system at a nominal hydrogen concentration $c_0 = 0.1$, temperature 300 K and distance $6b$.

increase of the moduli with hydrogen concentration [see (19)]. Since the hydrostatic stress elevation due to the modulus effect is in opposition to the hydrostatic stress relaxation due to the volumetric effect, the combined modulus and volumetric effects result in a hydrogen-induced stress, τ_H, larger in magnitude than the one associated with the volumetric field alone. In Fig. 12 the shear stress, τ_H, due to the combined effects is plotted against the normalized distance between the dislocations, l/b. The volumetric effect and the combined modulus and volumetric effects are compared in Fig. 13, where the percent reduction of the dislocation shear stress, τ_D, due to hydrogen is plotted against distance l/b.

Larche and Cahn (1985) have developed a formalism for treating the interactions of stress and composition. In contrast to the present treatment, which accounts for the local modulus change on a pointwise basis utilizing the local stress and solute concentration, that of Larche and Cahn (1985) relates the global moduli to the average solute concentration and the change of moduli with solute concentration evaluated at zero stress. Calculations of interactions between parallel edge dislocations carried out using the theory of Larche and Cahn (1985) are shown in Fig. 13. At large dislocation separations, the Larche and Cahn based calculations agree closely with the present results at low hydrogen concentrations. However, a significant underestimation of the effects of hydrogen occurs at small separations if the Larche and Cahn (1985) treatment is used, even at low concentrations of hydrogen. At the higher hydrogen concentrations, the Larche and Cahn (1985) treatment results in a significant

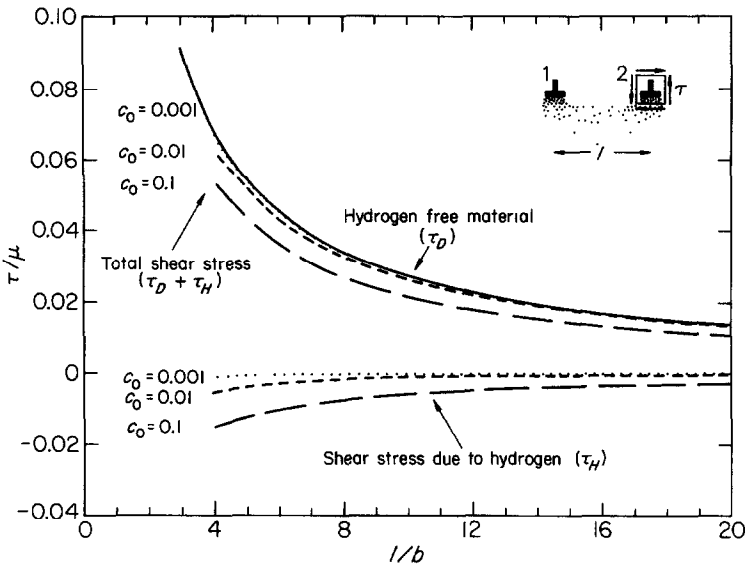

Fig. 12. Effect of the hydrogen-induced modulus change and relaxation of the hydrostatic stress on the normalized shear stress, τ_H/μ, due to hydrogen plotted versus dislocation distance, l/b, at temperature 300 K and nominal hydrogen concentrations of H/M = 0.1, 0.01 and 0.001. Stress, τ_D/μ, due to dislocation 1 and the net shear stress, $(\tau_D+\tau_H)/\mu$, are also shown.

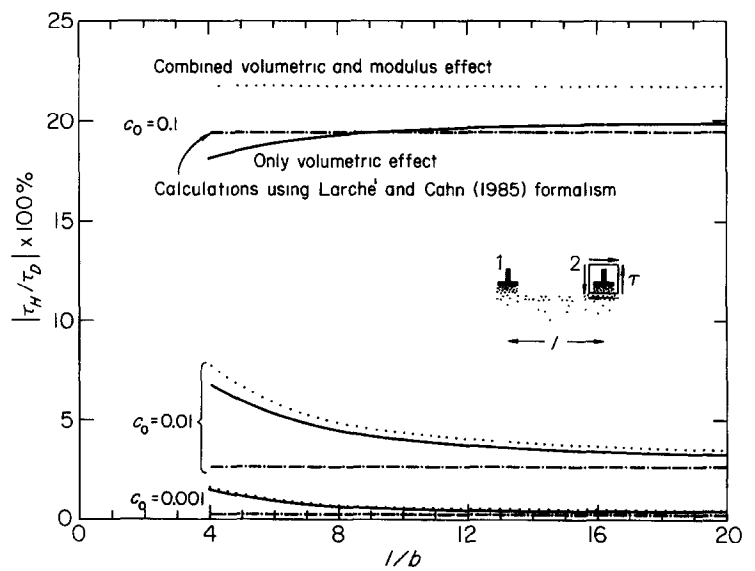

Fig. 13. Comparison of the volumetric effect with the combined modulus and volumetric effect on the percent reduction of the shear stress, τ_D, due to dislocation 1 in the absence of hydrogen at temperature 300 K. Calculations based on Larche and Cahn (1985) are also shown.

underestimation of the effects of hydrogen on dislocation interactions at all separations.

2.3. *Discussion of the results*

Both the analytical and finite element results of this work indicate that the hydrogen shielding effect reduces the repulsive force acting on parallel edge dislocations with Burgers vectors of the same sign on a glide plane. The reduction is a synergistic effect associated with the volumetric strain produced by the introduction of hydrogen into the lattice (volumetric effect) and the hydrogen induced changes in the constitutive moduli (modulus effect). The magnitude of these effects will depend on the nature of the variation of the moduli with hydrogen and, in the present paper, the case of increasing shear modulus with increased H/M is explored. The hydrogen-related decrease of the repulsive interaction depends strongly on the nominal hydrogen concentration, as indicated by Figs 5, 10, 12 and 13, and both volumetric and modulus effects on the absolute magnitude of the hydrogen-induced shear stress become weaker with increased dislocation separation. For dislocation separations greater than about 10 Burgers vectors, the percentage net stress reduction, i.e. the hydrogen stress normalized by the corresponding repulsive shear stress in the absence of hydrogen, is almost independent of the distance between the dislocations (see Fig. 13). At large dislocation separations, the total amount of hydrogen in the dislocation atmospheres responsible for the magnitude of the effect is almost independent of the dislocation separation and hence the normalized reduction is independent of dislocation separation.

It is important to recognize that these calculations were carried out under quasi-static "local equilibrium" conditions. Redistribution of the H solutes occurs within the solid over distances comparable to the dislocation separations, allowing H solute atmosphere equilibration with the far field H concentration. Since the far field concentration was maintained to C_0 the calculation corresponds to a constant chemical potential for the H. Dynamic effects on the solute atmosphere effects were not considered.

Hydrogen shielding of the stress fields of parallel edge dislocations results in a decrease in the magnitude of the shear stress, τ_D, which the dislocation 1 exerts on dislocation 2. As a consequence, the force between parallel dislocations is reduced, both for the repulsive force between two dislocations of the same sign and for the attractive force between two dislocations of opposite signed Burgers vectors. As expected from the hydrogen contribution to these interactions, the effects are greatest at small distances between the dislocations. The consequences of these effects on the dislocation behavior are many and only a few examples are cited below.

(a) Qualitatively, it is evident that in the presence of hydrogen, the spacing between dislocations in pile-ups will be decreased, particularly for the closely spaced dislocations at the tip of the pile-up. At sufficiently high H/M values and at close enough dislocation spacing, the sign of the force may in fact reverse and opposite signed dislocations can attract, causing fracture by the coalescence of edge dislocations at the head of the pile-up, a mechanism first proposed by Zener (1948) and discussed by Stroh (1957). (b) The internal stress field of plastically deformed metals is mainly

provided by the stress fields of dislocations and groups of dislocations. The general effect of hydrogen is to reduce these stresses and hence may be expected to reduce the internal stress field and the fluctuations in this field. Since in the deformed metals the mobility of dislocations is determined by the interaction of the moving dislocations with the internal stress field, the effect of a decrease in the internal stresses due to hydrogen is to decrease the barriers to dislocation motion and hence to increase the dislocation mobility. (c) Another consequence of the reduction of attractive interactions between opposite signed Burgers vectors is the decrease in stability of the dislocation dipoles formed during deformation, resulting in a decrease in the strength of these obstacles to dislocation motion.

3. HYDROGEN EFFECT ON THE INTERACTION BETWEEN A DISLOCATION AND AN IMPURITY ATOM

Interstitial solutes in BCC crystals are known to provide barriers to the motion of dislocation lines as they move through the crystal under the action of an applied stress. Cochardt *et al.* (1955) have studied the interaction between dislocations and interstitial solute atoms on the basis of the tetragonal distortion of the BCC lattice caused by carbon interstitials in alpha iron. In this section the effects of hydrogen on these interactions will be studied.

According to Cochardt *et al.* (1955), in the case of alpha iron the components of the transformation strain for a carbon interstitial having its tetragonal strain axis along the [100] axis of the crystal coordinate system are given by

$$[\boldsymbol{\varepsilon}^{TC}]_{ij} = \begin{bmatrix} \varepsilon_1 & 0 & 0 \\ 0 & \varepsilon_2 & 0 \\ 0 & 0 & \varepsilon_3 \end{bmatrix}, \tag{23}$$

where

$$\varepsilon_1 = 0.38, \quad \varepsilon_2 = \varepsilon_3 = -0.026, \tag{24}$$

and the strain is taken over the unit cell with lattice parameter a. The transformation strain due to interstitials having their tetragonal axes in directions [010] and [001] can be found by rearranging the components of $\boldsymbol{\varepsilon}^{TC}$ so that they are compatible with the corresponding distortion of the lattice.

3.1. *Edge dislocation*

3.1.1. *Formulation of the boundary value problem.* The net stress field in the lattice can be found by linear superposition of the fields of the hydrogen atmosphere, $\boldsymbol{\sigma}_H$, the carbon atom, $\boldsymbol{\sigma}_c$, and the dislocation, $\boldsymbol{\sigma}_D$. First, the combined stress field of the continuously distributed hydrogen and that of a single carbon interstitial in the absence of the dislocation, $\boldsymbol{\sigma}_H + \boldsymbol{\sigma}_C$ (carbon/hydrogen), is evaluated through the transformation strain model for carbon and hydrogen interstitials by accounting for the hydrogen-induced changes in the elastic moduli. The calculation of the combined

hydrogen and carbon field is carried out as in Section 2.2 with respect to a portion S of the hydrogen atmosphere, which in this case is taken to be circular and centered at the dislocation core. The external boundary, s, of area S is located remote from both the dislocation and the carbon interstitial and is traction free. Hydrogen solutes inside S induce a continuously varying dilatational transformation strain field which depends on the local hydrogen concentration as described by (17). The carbon interstitial induces a transformation strain given by (23) and (24) which is assigned to the point at which the carbon atom is located. Since hydrogen interacts with the tetragonal distortion of the carbon interstitial, the hydrogen concentration is calculated using an interaction energy based on the hydrostatic stress fields of the other hydrogen solutes, the carbon itself and the dislocation. Solution to this problem requires iteration, as has been discussed in Section 2.2. The stress field due to carbon, $\boldsymbol{\sigma}_C$, is then calculated by considering the carbon transformation strain fixed at the same position inside the region S in the absence of the dislocation and the hydrogen solutes (carbon/no-hydrogen). The external circular boundary of the region S is again traction free and its elastic moduli vary pointwise as dictated by the distribution of hydrogen in the combined carbon/hydrogen problem. The carbon/no-hydrogen problem is linear and can be solved directly.

Both stress fields of the combined carbon/hydrogen problem, and that of the carbon/no-hydrogen, are analysed in plane strain deformation conditions. Consider a Cartesian coordinate system x_1, x_2, x_3 centered at the dislocation core with the x_3 axis lying along the dislocation line in the [211] direction of the unit cell and the Burgers vector lying along the $[\bar{1}11]$. The domain S is identified with a circular region on the plane x_1–x_2. Using (23), one may find the unit cell components of the carbon transformation strain tensor with respect to the system of axes x_1, x_2, x_3 as

$$[\boldsymbol{\varepsilon}^{CT}]_{ij} = \begin{bmatrix} \frac{1}{3}(\varepsilon_1+\varepsilon_2+\varepsilon_3) & \frac{1}{\sqrt{6}}(\varepsilon_3-\varepsilon_2) & 0 \\ \frac{1}{\sqrt{6}}(\varepsilon_3-\varepsilon_2) & \frac{1}{2}(\varepsilon_2+\varepsilon_3) & 0 \\ 0 & 0 & \frac{2}{3}\varepsilon_1+\frac{1}{6}(\varepsilon_2+\varepsilon_3) \end{bmatrix}, \tag{25}$$

where strains ε_{13}^{CT} and ε_{23}^{CT} have been set equal to zero, since under plane strain conditions they do not affect the interaction of hydrogen with the stress field of the dislocation nor with the stress field of the hydrogen solutes. In accord with the plane strain deformation, the carbon mechanical effect can be thought of as arising from an infinite sequence of unit cubic cells all containing carbon atoms and aligned along an axis which is parallel to the x_3 axis. It is assumed that this infinitely long parallelepiped of unit cells intersects the x_1–x_2 plane over a plane domain S_c whose area is given by a_c^2, where a_c is a typical length scale of S_c. In the continuum plane strain model of the carbon-induced distortion domain, S_c is taken to represent an area which undergoes a transformation strain due to carbon. The magnitude of the transformation strain inside S_c can be calculated as follows: the unconstrained volume change of a unit cell in the cylinder-in-hole model equals $\varepsilon_{kk}^{CT}a^3$. Hence, the unit length of the parallelepiped which contains $1/a$ unit cells exhibits an unconstrained volume

change equal to $\varepsilon_{kk}^{CT}a^2$. Assuming this volume change, $\varepsilon_{kk}^{CT}a^2$, to be induced by an area expansion in the x_1–x_2 plane, one finds an unconstrained area change per unit length equal to $\varepsilon_{kk}^{CT}a^2$. A volumetric transformation strain, $\boldsymbol{\varepsilon}^C$, consistent with this area change may then be derived by equating $\varepsilon_{kk}^{CT}a^2$ to $\varepsilon_{kk}^{C}a_c^2$. Thus, under plane strain deformation conditions, the carbon lattice distortion is modeled through the area S_c, which undergoes a uniform transformation strain, $\boldsymbol{\varepsilon}^C$, such that

$$\varepsilon_{ij}^{C} = \left(\frac{a}{a_c}\right)^2 \varepsilon_{ij}^{CT} \tag{26}$$

in the system of x_1, x_2, x_3 axes.

The governing equations for both carbon/hydrogen and carbon/no-hydrogen problems are given in plane strain by (21) and (22) with volume V replaced by area S,

$$\varepsilon_{ij}^{T} = \begin{cases} \varepsilon_{ij}^{C} & \text{in} \quad S_c \\ \varepsilon_{ij}^{H} & \text{in} \quad S - S_c \end{cases} \tag{27}$$

for the carbon/hydrogen problem, and

$$\varepsilon_{ij}^{T} = \begin{cases} \varepsilon_{ij}^{C} & \text{in} \quad S_c \\ 0 & \text{in} \quad S - S_c \end{cases} \tag{28}$$

for the carbon/no-hydrogen problem.

3.1.2. *Results and interaction energy.* Solutions to both problems were found by a finite element method (Sofronis and Birnbaum, 1993) with the carbon atom position taken at the centroid of an element. The corresponding element area was identified with area S_c, which was assigned to undergo a uniform strain transformation $\boldsymbol{\varepsilon}^C$ determined through (26) with a_c^2 set equal to the element area. The finite element equations for the combined carbon/hydrogen problem were solved by the iterative technique described in Section 2.2.

First solutions were obtained for the carbon/no-hydrogen problem with the moduli taken constant and equal to those of the hydrogen-free material. The carbon area S_c was fixed on the x_1–x_2 plane at position (r, ϕ) relative to the dislocation at the origin. By averaging the shear stress σ_{12} around the origin, one finds the shear stress, τ, an edge dislocation would experience on its slip system if it were introduced at the origin in the absence of hydrogen. The interaction energy per unit length between the dislocation and the carbon atom can be found through

$$W = -\int_{S_c} (\sigma_D)_{ij}\varepsilon_{ij}^{C}\, dS, \tag{29}$$

where $(\sigma_D)_{ij}$ are the components of the singular dislocation stress field, σ_D (Hirth and Lothe, 1982). Using (25) and (26), one can evaluate the surface integral in (29) numerically. Results at various carbon atom positions relative to the dislocation were compared with the analytic solution (Cochardt *et al.*, 1955)

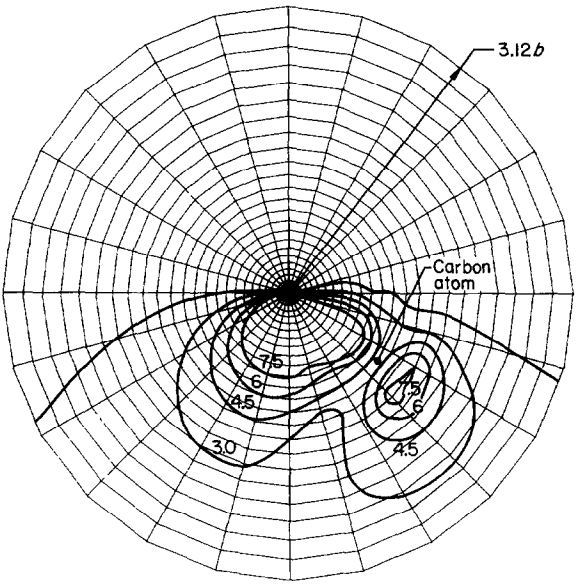

Fig. 14. Contours of normalized hydrogen concentration c/c_0 around an edge dislocation and a carbon atom with a tetragonal axis [001] at $r/b = 1.2$, $\phi = -37.5°$ relative to the dislocation in niobium at nominal hydrogen concentration $c_0 = 0.1$ and temperature 300 K. Both hydrogen effects (modulus and volumetric) were accounted for.

$$\tau = -\frac{Da^2}{r^2 b}\left\{\tfrac{1}{3}(\varepsilon_1+\varepsilon_2+\varepsilon_3)[(1+\nu)\sin 2\phi+\sin 4\phi]\right.$$
$$\left.-(\varepsilon_2+\varepsilon_3)\sin\phi\cos 3\phi-\frac{\sqrt{6}}{3}(\varepsilon_3-\varepsilon_2)\cos 4\phi+\nu\varepsilon_1\sin 2\phi\right\}, \quad (30)$$

$$W = -\frac{Da^2}{r}\left\{\tfrac{1}{3}\sin\phi(1+\nu+2\cos^2\phi)(\varepsilon_1+\varepsilon_2+\varepsilon_3)\right.$$
$$\left.-\tfrac{1}{2}(\varepsilon_2+\varepsilon_3)\sin\phi\cos 2\phi-\frac{\sqrt{6}}{3}\cos\phi\cos 2\phi(\varepsilon_3-\varepsilon_2)+\nu\varepsilon_1\sin\phi\right\}, \quad (31)$$

where $D = \mu b/[2\pi(1-\nu)]$, and excellent agreement was found (Sofronis and Birnbaum, 1993). This agreement indicates that the finite element solutions are very accurate, thereby implying that the plane strain model used for the carbon distortion field reliably simulates the mechanical behavior of the carbon interstitial.

The finite element solutions for the carbon/hydrogen problem provide the distribution of the hydrogen atoms around the dislocation and the carbon atom. A representative situation is shown in Fig. 14, where the solution for the iso-concentration lines was obtained by accounting for the hydrogen-induced modulus change. The calculation was carried out at nominal concentration of H/M = 0.1, with the carbon interstitial at position $r/b = 1.2$, $\phi = -37.5°$, the carbon tetragonal axis

in the [001] direction and the edge dislocation line along the [211] direction with its Burgers vector in the $[\bar{1}11]$.

The hydrogen effect is assessed by calculating the change in the interaction energy W between the dislocation and the carbon atom caused by the presence of hydrogen. According to (31), the stress fields of the edge dislocation and the carbon atom do not interact when the defects are at a sufficiently large distance apart. In that case, the atmospheres which form around the edge dislocation and the carbon atom, upon the introduction of hydrogen into the lattice, can be considered effectively identical to those that would form around each of the defects in the absence of the other. Upon the action of an external stress, the dislocation and its symmetric atmosphere (configuration A) can be brought close to the carbon atom and its hydrogen atmosphere (configuration B) so that the constituents of the configurations A and B begin to interact among one another. The result of this interaction is a configuration AB characterized by hydrogen redistribution around the two defects. The corresponding hydrogen atmosphere of configuration AB is furnished by a solution of the carbon/hydrogen problem. In bringing configurations A and B together, the assumption of an open system was introduced with fast diffusion relaxation rates. The hydrogen effect can be assessed by comparing the interaction energy W_H between configurations A and B to the interaction energy W in the absence of hydrogen as given by (31).

In the following, the dislocation stress field is calculated as in Hirth and Lothe (1982) but use is made of the linear elastic moduli as affected by the corresponding local hydrogen composition. An elastic state $(\boldsymbol{\sigma}, \mathbf{T}, \boldsymbol{\varepsilon}, \boldsymbol{\varepsilon}_{\text{elast}}, \boldsymbol{\varepsilon}^{\text{T}}, \mathbf{u})$ is defined over the region S loaded with tractions $\mathbf{T}$ along the boundary s by a transformation strain field $\boldsymbol{\varepsilon}^{\text{T}}$, an elastic strain field $\boldsymbol{\varepsilon}_{\text{elast}}$, a net strain field $\boldsymbol{\varepsilon} = \boldsymbol{\varepsilon}_{\text{elast}} + \boldsymbol{\varepsilon}^{\text{T}}$, and a displacement field $\mathbf{u}$ such that

$$\left.\begin{aligned} \sigma_{ij,j} &= 0 \\ \varepsilon_{ij} &= \tfrac{1}{2}(u_{i,j} + u_{j,i}) \\ \sigma_{ij} &= C_{ijkl}(\varepsilon_{kl} - \varepsilon^{\text{T}}_{kl}) \end{aligned}\right\} \text{in} \quad S$$
$$\sigma_{ij}\eta_j = T_i \qquad \text{on} \quad s. \tag{32}$$

When the configurations A and B interact, the final elastic state for configuration AB is found by linear superposition of states $(\boldsymbol{\sigma}_{\text{D}}, \mathbf{T}_{\text{D}}, \boldsymbol{\varepsilon} = \boldsymbol{\varepsilon}_{\text{D}}, \boldsymbol{\varepsilon}_{\text{elast}} = \boldsymbol{\varepsilon}_{\text{D}}, \boldsymbol{\varepsilon}^{\text{T}} = 0, \mathbf{u}_{\text{D}})$ of the dislocation, $(\boldsymbol{\sigma}_{\text{C}}, \mathbf{T}_{\text{C}} = 0, \boldsymbol{\varepsilon} = \boldsymbol{\varepsilon}^{(\text{C})}, \boldsymbol{\varepsilon}_{\text{elast}} = \boldsymbol{\varepsilon}_{\text{C}}, \boldsymbol{\varepsilon}^{\text{T}} = \boldsymbol{\varepsilon}^{\text{C}}, \mathbf{u}^{(\text{C})})$ of the carbon atom furnished by the solution to the carbon/no-hydrogen problem and $(\boldsymbol{\sigma}_{\text{H}}, \mathbf{T}_{\text{H}} = 0, \boldsymbol{\varepsilon} = \boldsymbol{\varepsilon}^{(\text{H})}, \boldsymbol{\varepsilon}_{\text{elast}} = \boldsymbol{\varepsilon}_{\text{H}}, \boldsymbol{\varepsilon}^{\text{T}} = \boldsymbol{\varepsilon}^{\text{H}}, \mathbf{u}^{(\text{H})})$ of the hydrogen atmosphere as calculated in the carbon/hydrogen problem. The elastic state for the dislocation is found after the carbon/hydrogen problem is solved and the elastic moduli are determined by the corresponding hydrogen concentration. By linear superposition the potential energy W(D,C,H) per unit length of configuration AB is given by

$$W(\text{D,C,H}) = \frac{1}{2}\int_S (\sigma_{\text{D}} + \sigma_{\text{C}} + \sigma_{\text{H}})_{ij}(\varepsilon_{\text{D}} + \varepsilon_{\text{C}} + \varepsilon_{\text{H}})_{ij}\,\text{d}S - \int_s (T_{\text{D}})_i(u_{\text{D}} + u^{(\text{C})} + u^{(\text{H})})_i\,\text{d}s, \tag{33}$$

where D stands for dislocation, C for carbon and H for hydrogen. In Appendix B it is shown that (33) may be cast into

$$W(\mathrm{D,C,H}) = -\frac{1}{2}\int_{S-S_{\mathrm{core}}} (\sigma_{\mathrm{D}})_{ij}(\varepsilon_{\mathrm{D}})_{ij}\,\mathrm{d}S - \frac{1}{2}\int_S (\sigma_{\mathrm{C}})_{ij}(\varepsilon^{\mathrm{C}})_{ij}\,\mathrm{d}S - \frac{1}{2}\int_S (\sigma_{\mathrm{H}})_{ij}(\varepsilon^{\mathrm{H}})_{ij}\,\mathrm{d}S$$
$$- \int_S (\sigma_{\mathrm{D}})_{ij}(\varepsilon^{\mathrm{C}})_{ij}\,\mathrm{d}S - \int_S (\sigma_{\mathrm{D}})_{ij}(\varepsilon^{\mathrm{H}})_{ij}\,\mathrm{d}S - \int_S (\sigma_{\mathrm{H}})_{ij}(\varepsilon^{\mathrm{C}})_{ij}\,\mathrm{d}S, \quad (34)$$

where S_{core} is the excluded core region of the dislocation. The elastic state for configuration A is found by linear superposition of state ($\boldsymbol{\sigma}_{\mathrm{DH}}$, $\mathbf{T}_{\mathrm{DH}}$, $\boldsymbol{\varepsilon} = \boldsymbol{\varepsilon}_{\mathrm{DH}}$, $\boldsymbol{\varepsilon}_{\mathrm{elast}} = \boldsymbol{\varepsilon}_{\mathrm{DH}}$, $\boldsymbol{\varepsilon}^{\mathrm{T}} = 0$, $\mathbf{u}_{\mathrm{DH}}$) for the dislocation in an infinite medium and state ($\boldsymbol{\sigma}_{\mathrm{HD}}$, $\mathbf{T}_{\mathrm{HD}} = 0$, $\boldsymbol{\varepsilon} = \boldsymbol{\varepsilon}^{(\mathrm{HD})}$, $\boldsymbol{\varepsilon}_{\mathrm{elast}} = \boldsymbol{\varepsilon}_{\mathrm{HD}}$, $\boldsymbol{\varepsilon}^{\mathrm{T}} = \boldsymbol{\varepsilon}^{\mathrm{HD}}$, $\mathbf{u}^{(\mathrm{HD})}$) for its symmetric atmosphere in the absence of the carbon interstitial. Both states are calculated by solving the carbon/hydrogen problem with the carbon area S_{C} taken to be occupied by hydrogen instead of the carbon atom. The stresses, strains and displacements in these two states of configuration A are different from the corresponding ones in configuration AB because the respective hydrogen atmospheres and consequently the elastic moduli are different. Similarly, by solving the carbon/hydrogen problem, one calculates the elastic state ($\boldsymbol{\sigma}_{\mathrm{HC}}$, $\mathbf{T}_{\mathrm{HC}} = 0$, $\boldsymbol{\varepsilon} = \boldsymbol{\varepsilon}^{(\mathrm{HC})}$, $\boldsymbol{\varepsilon}_{\mathrm{elast}} = \boldsymbol{\varepsilon}_{\mathrm{HC}}$, $\boldsymbol{\varepsilon}^{\mathrm{T}} = \boldsymbol{\varepsilon}^{\mathrm{HC}}$, $\mathbf{u}^{(\mathrm{HC})}$) for the hydrogen atmosphere around the carbon atom in the absence of the dislocation and its contribution to interaction energy W_{int} of (3), and the elastic state ($\boldsymbol{\sigma}_{\mathrm{CH}}$, $\mathbf{T}_{\mathrm{CH}} = 0$, $\boldsymbol{\varepsilon} = \boldsymbol{\varepsilon}^{(\mathrm{CH})}$, $\boldsymbol{\varepsilon}_{\mathrm{elast}} = \boldsymbol{\varepsilon}_{\mathrm{CH}}$, $\boldsymbol{\varepsilon}^{\mathrm{T}} = \boldsymbol{\varepsilon}^{\mathrm{C}}$, $\mathbf{u}^{(\mathrm{CH})}$) for the carbon atom alone in an infinite medium whose moduli have been changed by the hydrogen atmosphere of configuration B. Superposing these two elastic states, one finds the elastic state for configuration B. The potential energy for configuration A is computed from (33) by dropping the terms related to the carbon atom

$$W(\mathrm{D,H}) = -\frac{1}{2}\int_{S-S_{\mathrm{core}}} (\sigma_{\mathrm{DH}})_{ij}(\varepsilon_{\mathrm{DH}})_{ij}\,\mathrm{d}S - \frac{1}{2}\int_S (\sigma_{\mathrm{HD}})_{ij}(\varepsilon^{\mathrm{HD}})_{ij}\,\mathrm{d}S - \int_S (\sigma_{\mathrm{DH}})_{ij}(\varepsilon^{\mathrm{HD}})_{ij}\,\mathrm{d}S \quad (35)$$

and the potential energy for configuration B is computed by dropping the terms related to the dislocation

$$W(\mathrm{C,H}) = -\frac{1}{2}\int_S (\sigma_{\mathrm{CH}})_{ij}(\varepsilon^{\mathrm{C}})_{ij}\,\mathrm{d}S - \frac{1}{2}\int_S (\sigma_{\mathrm{HC}})_{ij}(\varepsilon^{\mathrm{HC}})_{ij}\,\mathrm{d}S - \int_S (\sigma_{\mathrm{HC}})_{ij}(\varepsilon^{\mathrm{C}})_{ij}\,\mathrm{d}S. \quad (36)$$

The interaction energy between configurations A and B is defined as

$$W_{\mathrm{H}} = W(\mathrm{D,C,H}) - W(\mathrm{D,H}) - W(\mathrm{C,H}) \quad (37)$$

and using (34)–(36) one finds

$$W_H = \frac{1}{2}\int_{S-S_{core}} (\sigma_{DH})_{ij}(\varepsilon_{DH})_{ij}\,dS - \frac{1}{2}\int_{S-S_{core}} (\sigma_D)_{ij}(\varepsilon_D)_{ij}\,dS$$
$$+\left(-\frac{1}{2}\int_S (\sigma_C)_{ij}(\varepsilon^C)_{ij}\,dS\right)-\left(-\frac{1}{2}\int_S (\sigma_{CH})_{ij}(\varepsilon^C)_{ij}\,dS\right)$$
$$+\left(-\frac{1}{2}\int_S (\sigma_H)_{ij}(\varepsilon^H)_{ij}\,dS\right)-\left(-\frac{1}{2}\int_S (\sigma_{HD})_{ij}(\varepsilon^{HD})_{ij}\,dS\right)-\left(-\frac{1}{2}\int_S (\sigma_{HC})_{ij}(\varepsilon^{HC})_{ij}\,dS\right)$$
$$-\int_S (\sigma_D+\sigma_H-\sigma_{HC})_{ij}(\varepsilon^C)_{ij}\,dS$$
$$+\left(-\int_S (\sigma_D)_{ij}(\varepsilon^H)_{ij}\,dS\right)-\left(-\int_S (\sigma_{DH})_{ij}(\varepsilon^{HD})_{ij}\,dS\right). \tag{38}$$

The first line in the right hand side of (38) represents the difference in the strain energy of the edge dislocation between configurations A and AB. The second line represents the difference in the strain energy of solution of the carbon interstitial between configurations B and AB. The three terms in the third line represent the strain energy of solution of hydrogen in configurations AB, A and B, respectively. The fourth line represents interaction energy between the dislocation in configuration AB, the hydrogen in configuration AB and the hydrogen in configuration B with the carbon atom. The last line represents the difference in the interaction energy of the edge dislocation with its hydrogen atmosphere between configurations AB and A. The formalism which led to (38) is not restricted only to the case of hydrogen studied, but can be applied for interaction energy calculations involving stresses caused by any distribution of stress centers.

The issue of whether to include the elastic strain energy [the terms in the third line of (38)] in the calculation of the interaction energy between the dislocation and the carbon atom in the presence of hydrogen solutes depends on whether the system is an "open" or "closed" system. An "open" system can exchange hydrogen with its thermodynamic reservoir, e.g. a gas phase, while a "closed" system is inhibited from doing so by kinetics, the presence of an impermeable oxide film, etc. Processes in which the interactions between the dislocation and elastic centers, such as carbon solutes, are rapid compared to the time for equilibrium of the solid with the hydrogen reservoir can be considered "pseudo-closed." In this case, the stress fields allow local rearrangements of the hydrogen solutes and concentrations without changing the overall hydrogen concentration in the solid by transfer of hydrogen across the external surfaces of the solid. In all of the previous calculations of the interaction stresses between the dislocations and the stress centers, the system was "closed" or "pseudo-closed" and local equilibration of the hydrogen concentration was allowed. An explicit choice must be made in the calculation of the elastic interaction energies as the terms in the third line must be included for an "open" system but not for a "closed" or "pseudo-closed" system. In these latter cases, the total amount of hydrogen in the system remains constant. It should also be noted that the terms in the third line of (38) account only for the strain energy portion of the energy of solution of hydrogen

and that, in general, the strain energy is only a small component of the total energy of solution.

In the present paper, the solution strain energy terms will not be considered in calculating the interaction energies between dislocations and elastic strain centers in the presence of hydrogen. This is appropriate for considerations of the effects of hydrogen on deformation and fracture, as many systems have barriers to equilibrium with the ambient. In addition, the times appropriate to describe the interactions of dislocations with defects are very small compared to the equilibration times for solution of hydrogen from the gas phase. The stress effects on the total hydrogen concentration in the specimen [third line of (38)] are appropriate in discussing the effects of dislocations in the solubility of hydrogen in equilibrium with a reference state (Flannagan *et al.*, 1981; Kirchheim, 1986).

Notice that in the absence of hydrogen, only the first term in the fourth line survives and the result is identical to that of (29). In the presence of hydrogen, neglect of the change in elastic moduli due to hydrogen and the strain energy of solution of hydrogen results in a modification of (38) to yield for the interaction energy

$$W'_{\mathrm{H}} = -\int_S (\sigma_{\mathrm{D}}+\sigma_{\mathrm{H}}-\sigma_{\mathrm{HC}})_{ij}(\varepsilon^{\mathrm{C}})_{ij}\,\mathrm{d}S+\left(-\int_S (\sigma_{\mathrm{D}})_{ij}(\varepsilon^{\mathrm{H}})_{ij}\,\mathrm{d}S\right) -\left(-\int_S (\sigma_{\mathrm{DH}})_{ij}(\varepsilon^{\mathrm{HD}})_{ij}\,\mathrm{d}S\right). \quad (39)$$

The calculation of the interaction energy W_{H} in (38) is insensitive to the magnitude of the core area when the core cut-off radius is sufficiently small. For a small cut-off radius, stresses close to the core are sufficiently high to allow the tensile side of the dislocation to be saturated with hydrogen and the compressive side to be significantly depleted of hydrogen in configurations A and AB. In that case the region very close to the core exhibits the same elastic moduli in configurations A and AB and consequently the elastic strain energy associated with the dislocation singular stress field of that region is also the same for configurations A and AB. As a result, the corresponding contribution of the near core regions to the difference in the dislocation strain energy in (38) is zero. Hydrogen concentrations calculated within a radius $0.02b$ around the origin were always found to be at hydrogen saturation levels on the tensile side of the core and zero on the compressive side.

In Figs 15–17 the interaction energy per interatomic distance aW, between the dislocation and the carbon atom having the tetragonal axes in directions [100], [010] and [001], in the absence of hydrogen, is plotted against the carbon atom position x_1/b, $x_2/b = -0.505$ relative to the dislocation, which is fixed at the origin of the coordinate system. Energy aW is measured in eV per slab of thickness a and is calculated using (31). The same figures show the results of calculations in the presence of hydrogen for the interaction energy aW'_{H} calculated by (39) with neglect of the modulus effect, and the interaction energy aW_{H} calculated using (38) taking account of the modulus effect. Figures 15–17 demonstrate a negative interaction energy when the dislocation approaches the carbon interstitial, as expected. The presence of hydrogen reduces the strength of the interaction, with the effect being greater if the modulus effect is included in the calculation.

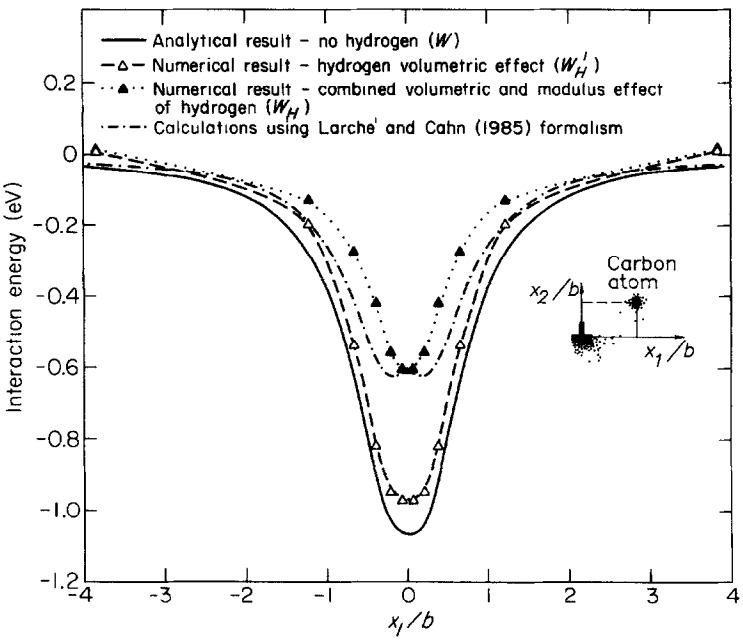

Fig. 15. Plot of the edge dislocation–carbon atom interaction energy measured in eV per slab of thickness a versus carbon atom position x_1/b, $x_2/b = -0.505$ relative to the dislocation for a carbon atom with a tetragonal axis [100]. The hydrogen effect was calculated at temperature 300 K and nominal hydrogen concentration of H/M = 0.1.

Calculations based on the Larche and Cahn (1985) treatment of the effects of solutes on elastic interactions are included in Figs 15–17. In some cases (Fig. 15) the global treatment of the solute effect gives approximate agreement with the present calculations, while in others it significantly underestimates the hydrogen effects at the crucially important small values of x_1/b. The full pointwise calculation results in a significantly greater diminution of the interaction energy than does the global approach of Larche and Cahn (1985).

To examine the dependence of the hydrogen effect on the distance x_2/b of the carbon atom from the slip plane, calculations with $x_2/b = -3.046$ were carried out. Results typical of the behavior at this larger separation are shown in Fig. 18, where the interaction energies aW, aW'_{H} and aW_{H} are plotted against the carbon atom position x_1/b relative to the dislocation. The carbon atom occupied the interstitial position having a [010] tetragonal axis and the nominal H/M ratio was 0.1. As shown by comparing Figs 16 and 18, at large dislocation–carbon separations the presence of hydrogen increases the magnitude of the interaction energy slightly and alters the shape and position of the interaction relative to the solution in the absence of hydrogen, in contrast to the effects at smaller dislocation–carbon separations. Figure 18 also shows that the modulus effect becomes relatively unimportant when the dislocation and the carbon atom are at distance greater than about three Burgers vectors. Since the force exerted by the C solute on the dislocation is given by the slope of the interaction curves, in Fig. 18 it is seen that at large values of x_2/b, hydrogen sig-

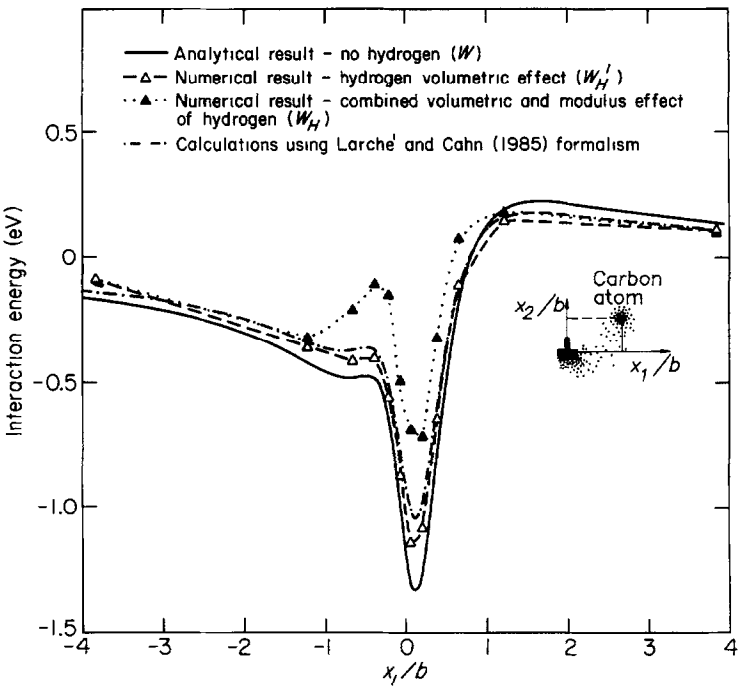

Fig. 16. Plot of the edge dislocation–carbon atom interaction energy measured in eV per slab of thickness a versus carbon atom position x_1/b, $x_2/b = -0.505$ relative to the dislocation for a carbon atom with a tetragonal axis [010]. The hydrogen effect was calculated at temperature 300 K and nominal hydrogen concentration of H/M = 0.1

nificantly decreases the force on the dislocation for $x_1/b < 0$, in contrast to the small effect of hydrogen on the interaction force at small values of x_2/b. At these larger separations of the C interstitial from the dislocation slip plane, the global modulus change treatment of Larche and Cahn (1985) (Fig. 18) gives a result greatly at variance with the present calculations.

3.1.3. *Discussion of the results.* The results shown in Figs 15–17 are consistent with the well known phenomenon of the dislocation motion hindered by impurity atoms. The pinning of dislocations by interstitial solutes such as carbon results from a negative interaction energy when the defects are very close to each other. The addition of hydrogen to the system decreases the magnitude of this negative interaction energy, thereby diminishing the ability of the solute atoms to pin the dislocations. As discussed previously, the present calculations take only the first order elastic interaction energy between the dislocation and the hydrogen solutes into account in calculating the H/M values near the dislocation. In general, the second order elastic interaction, due to hydrogen effects on the elastic moduli, is considerably less significant in determining the H/M values near the dislocation than the first order interaction, due to the elastic distortion field around the hydrogen, and is ignored in the present calculation. This second order elastic effect will be considered in a subsequent paper as it may make a significant contribution when the important interactions are close to the dislocation

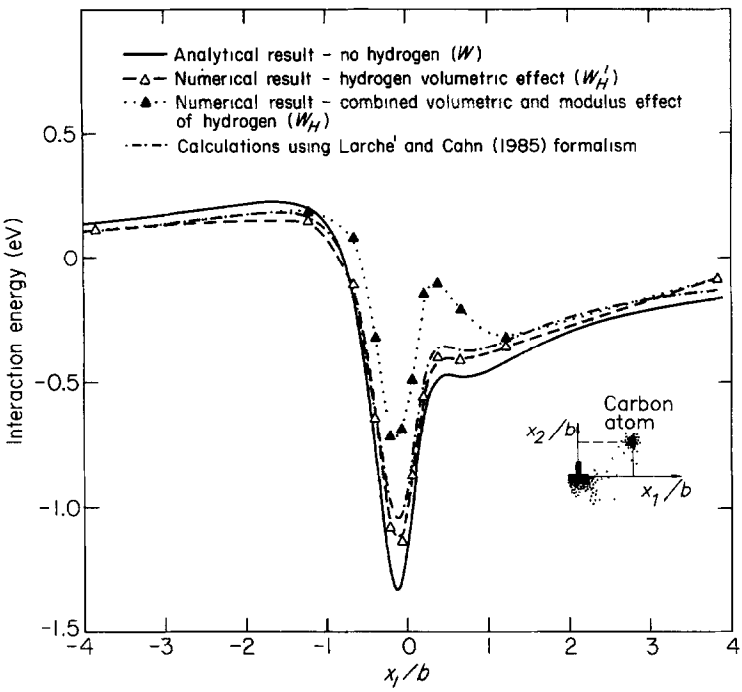

Fig. 17. Plot of the edge dislocation–carbon atom interaction energy measured in eV per slab of thickness a versus carbon atom position x_1/b, $x_2/b = -0.505$ relative to the dislocation for a carbon atom with a tetragonal axis [001]. The hydrogen effect was calculated at temperature 300 K and nominal hydrogen concentration of H/M = 0 1

core, as in the present case of the dislocation–C–hydrogen interactions and when the shear modulus decreases as H/M increases, leading to a negative value of $W_{\text{int}}^{(2)}$ and an increase in the H/M values close to the dislocation.

The calculated interactions between the edge dislocations and point defects and the influence of hydrogen on these interactions (Figs 15–17) are in excellent agreement with the experimental measurements on the Ni–C–H system (Sirois and Birnbaum, 1992). Hydrogen was shown to decrease the "activation enthalpy" for slip (corresponding to the decrease in the calculated interaction energy with hydrogen) and to decrease the "activation volume" (corresponding to the decrease in the width of the activation energy minimum). The magnitude and nature of the hydrogen effect depends strongly on the distance between the defects. Figures 15–18 show that the hydrogen effect is significant in weakening the interaction only when the dislocation slip plane–carbon distance is approximately less than $2b$. For defect distances greater than $2b$, the magnitude of the interaction energy is relatively unaffected by the presence of hydrogen. The force–displacement profile for the pinning interaction is markedly changed by hydrogen for dislocation slip plane–carbon distances of $2b$ or greater and is unaffected by hydrogen for distances of less than $2b$. The same insensitivity of the interaction energy to the presence of hydrogen was observed when the edge dislocation slip plane was $3b$ below the carbon atom, i.e. when the carbon solute was in the compressive stress field.

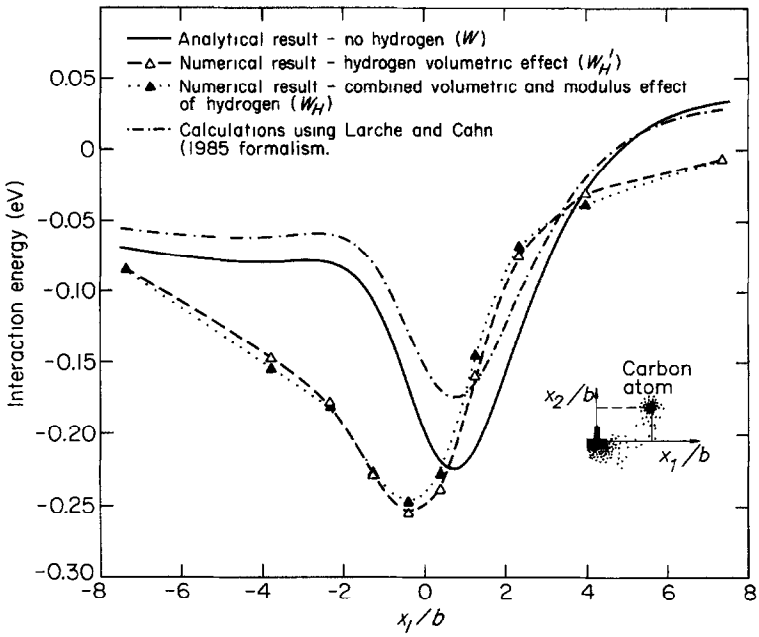

Fig. 18. Plot of the edge dislocation–carbon atom interaction energy measured in eV per slab of thickness a versus carbon atom position x_1/b, $x_2/b = -3.046$ relative to the dislocation for a carbon atom with a tetragonal axis [010]. The hydrogen effect was calculated at temperature 300 K and nominal hydrogen concentration of H/M = 0.1.

Figures 15–18 indicate that at dislocation slip plane–defect distances less than $2b$ the hydrogen-induced weakening of the interaction is predominantly due to the effect of hydrogen on the elastic moduli. Figure 18 shows that at distance greater than $3b$ the modulus effect causes almost no change to the interaction energy, compared to that caused by the dilatational effect. The local character of the modulus effect is in accordance with the same observation for the dislocation–dislocation interaction discussed in Section 2.3. It is worth noting, though, that at a nominal concentration of H/M = 0.1, the modulus effect on the dislocation–dislocation interaction was nearly independent of the defect distance (see Fig. 13), while in the case of the carbon–dislocation system the effect does exhibit a dependence on the defect separation, particularly when it is less than $2b$. This can be attributed to the continuous modification of the shape and relative position of the hydrogen iso-concentration curves, and in turn of those of the elastic moduli, as the dislocation passes above the carbon atom whose distortion field is not symmetric.

3.2. *Screw dislocation*

3.2.1. *Interaction energy in the absence of hydrogen.* Consider Cartesian coordinates x_1, x_2, x_3 with axis x_3 parallel to the dislocation line along the [111] direction of the unit cell in a BCC lattice. Choose axis x_1 parallel to the direction $[2\bar{1}\bar{1}]$ which is the projection of the 1-axis of the cell in the plane normal to the dislocation (x_1–x_2 plane). The carbon atom position in the vicinity of the dislocation can be described by

cylindrical polar coordinates (r, ϕ, x_3) with the angle ϕ measured from the positive x_1 axis. Using the rule of transformation of axes and (25), one finds the components of the carbon transformation strain tensor in system x_1, x_2, x_3 as

$$[\varepsilon^{CT}]_{ij} = \begin{bmatrix} \frac{1}{6}(4\varepsilon_1+\varepsilon_2+\varepsilon_3) & \frac{1}{\sqrt{12}}(\varepsilon_3-\varepsilon_2) & \frac{1}{\sqrt{18}}(2\varepsilon_1-\varepsilon_2-\varepsilon_3) \\ \frac{1}{\sqrt{12}}(\varepsilon_3-\varepsilon_2) & \frac{1}{2}(\varepsilon_2+\varepsilon_3) & \frac{1}{\sqrt{6}}(\varepsilon_2-\varepsilon_3) \\ \frac{1}{\sqrt{18}}(2\varepsilon_1-\varepsilon_2-\varepsilon_3) & \frac{1}{\sqrt{6}}(\varepsilon_2-\varepsilon_3) & \frac{1}{3}(\varepsilon_1+\varepsilon_2+\varepsilon_3) \end{bmatrix}. \tag{40}$$

With respect to the same system, the stress components of the anti-plane dislocation strain field are given in Hirth and Lothe (1982) as

$$[\sigma_D]_{ij} = \frac{\mu b}{2\pi r}\begin{bmatrix} 0 & 0 & -\sin\phi \\ 0 & 0 & \cos\phi \\ -\sin\phi & \cos\phi & 0 \end{bmatrix}. \tag{41}$$

Equations (40) and (41) can be used to calculate the interaction energy per slab of thickness a between the dislocation and the carbon interstitial atom,

$$aW = -\int_{V_{cell}} (\sigma_D)_{ij}(\varepsilon^{TC})_{ij}\,dV \tag{42}$$

$$= -a^3\frac{\mu b}{6\pi r}[\sqrt{6}(\varepsilon_2-\varepsilon_3)\cos\phi - \sqrt{2}(2\varepsilon_1-\varepsilon_2-\varepsilon_3)\sin\phi],$$

where V_{cell} is the volume of the unit cell. It is worth noting that (42) for the interaction energy differs from the corresponding relation

$$aW = \frac{\sqrt{2}b\mu a^3}{3\pi}(\varepsilon_1-\varepsilon_2)\frac{\cos\theta}{r} \tag{43}$$

given by Cochardt *et al.* (1955), with θ defined as the fixed angle between their x_1 axis, labeled as x', and the $[2\bar{1}\bar{1}]$ direction. Their relation, (43), appears to be in error as it suggests an interaction energy dependent on the choice of the x' coordinate axis, and does not account for the dependence of the interaction energy upon the relative angular position between the carbon atom and the screw dislocation.

3.2.2. *Hydrogen effect.* The purely deviatoric stress field of the screw dislocation implies, to first order, that there is no interaction between the dislocation and the hydrostatic distortion due to hydrogen atom. In the present calculation, the modulus effect on W_{int} for the evaluation of the hydrogen concentration field around the screw dislocation through (3) was neglected. Therefore, the amount of hydrogen in configuration A is unaffected by the presence of the screw dislocation and the hydrogen concentration remains uniform in space and equal to the nominal concentration C_0. Moreover, as the screw dislocation approaches configuration B, and begins to interact

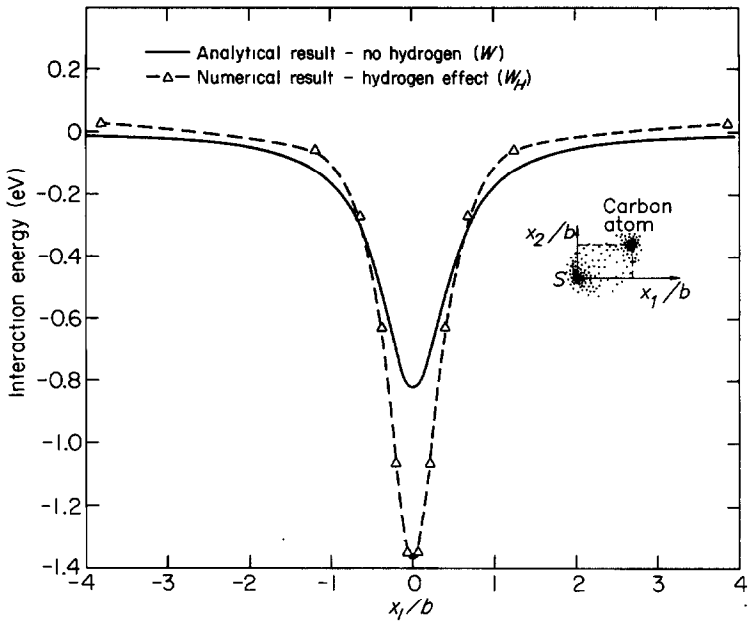

Fig. 19. Plot of the screw dislocation–carbon atom interaction energy measured in eV per slab of thickness a versus carbon atom position x_1/b, $x_2/b = -0.505$ relative to the dislocation for a carbon atom with a tetragonal axis [100]. The hydrogen effect was calculated at temperature 300 K and nominal hydrogen concentration of H/M = 0.1.

with the carbon atom according to (42), the hydrogen atmosphere in configuration B is not affected by the stress of the screw dislocation. Therefore, any changes to the interaction energy W given by (42) are associated with the local modulus change in configuration B, i.e. with the carbon interstitial and its hydrogen atmosphere. In view of this discussion, the interaction energy between configurations A and B was calculated using (38),

$$W_{\mathrm{H}} = W + \frac{1}{2}\int_{S - S_{\mathrm{core}}} (\sigma_{\mathrm{DA}})_{ij}(\varepsilon_{\mathrm{DA}})_{ij}\,\mathrm{d}S - \frac{1}{2}\int_{S\ \ S_{\mathrm{core}}} (\sigma_{\mathrm{D}})_{ij}(\varepsilon_{\mathrm{D}})_{ij}\,\mathrm{d}S. \tag{44}$$

The second term on the right hand side represents the strain energy of the screw dislocation in configuration A calculated as in Hirth and Lothe (1982) with the shear modulus evaluated by (19) at nominal hydrogen concentration C_0, whereas the third term represents the strain energy of the dislocation accounting for the pointwise induced modulus change by the hydrogen atmosphere of the carbon atom. The hydrogen atmosphere in configuration B and the associated local constitutive moduli were calculated by solving the carbon/hydrogen problem, as in Section 3.1, with zero contribution from the dislocation stress field to the interaction energy W_{int} of (3). This is a plane strain calculation where the carbon transformation strains $\varepsilon^{\mathrm{C}}_{ij}$ of (26) were found by using (40) with $\varepsilon^{\mathrm{CT}}_{13} = \varepsilon^{\mathrm{CT}}_{23} = 0$. This modification of the carbon transformation strain may be justified on the grounds that components $\varepsilon^{\mathrm{CT}}_{13}$ and $\varepsilon^{\mathrm{CT}}_{23}$ are out-of-plane shear strains and as such they do not interact with hydrogen.

3.2.3. *Results and discussion.* In Figs 19–21 the interaction energies aW and aW_{H}

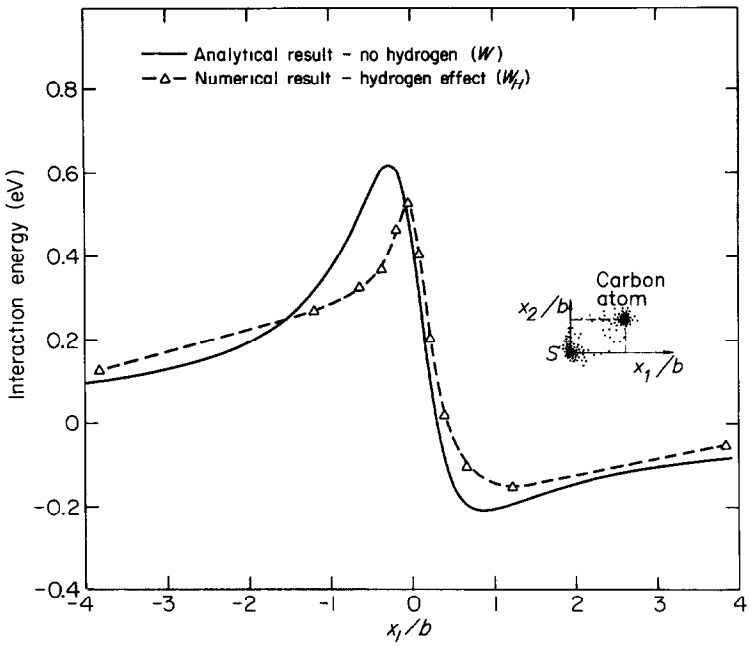

Fig. 20. Plot of the screw dislocation–carbon atom interaction energy measured in eV per slab of thickness a versus carbon atom position x_1/b, $x_2/b = -0.505$ relative to the dislocation for a carbon atom with a tetragonal axis [010]. The hydrogen effect was calculated at temperature 300 K and nominal hydrogen concentration of H/M = 0.1.

per slab of thickness a between the screw dislocation and carbon atoms having their tetragonal axes along directions [100], [010] and [001] respectively are plotted against its position x_1/b, $x_2/b = -0.505$ relative to the dislocation, which is fixed at the origin of the coordinate system. The temperature was 300 K and the nominal hydrogen concentration was H/M = 0.1. As before with phenomena resulting from the second order modulus interaction, the hydrogen effect is significant only for dislocation–defect separations of approximately less than about two Burgers vectors. Figure 19 shows that for [100] occupancy hydrogen increases the magnitude of the interaction of the screw dislocation with the carbon atom, thereby enhancing the latter's capability to hinder the dislocation motion. The equilibrium position is at $x_1/b = 0$. Figure 20 shows that for [010] occupancy, hydrogen does not affect the dislocation motion from position $x_1/b = 4$ towards the carbon atom at $x_1/b = 0$. However, the hydrogen reduces the energy barrier for the dislocation to move from the equilibrium position at $x_1/b \approx 0$ to negative values of x_1/b. Hydrogen thus facilitates the motion of the dislocation to negative x_1/b values, introducing an asymmetry in the hydrogen softening. For [001] occupancy, Fig. 21 indicates a similar asymmetry in the hydrogen-related decrease in the interaction energy, with the reduced interaction being in the region $x_1/b > -1$.

It is in the case of the screw dislocation–C–hydrogen interaction that the second order elastic interaction between the screw dislocation and the hydrogen solutes is expected to be the most significant. Since there is no first order elastic interaction

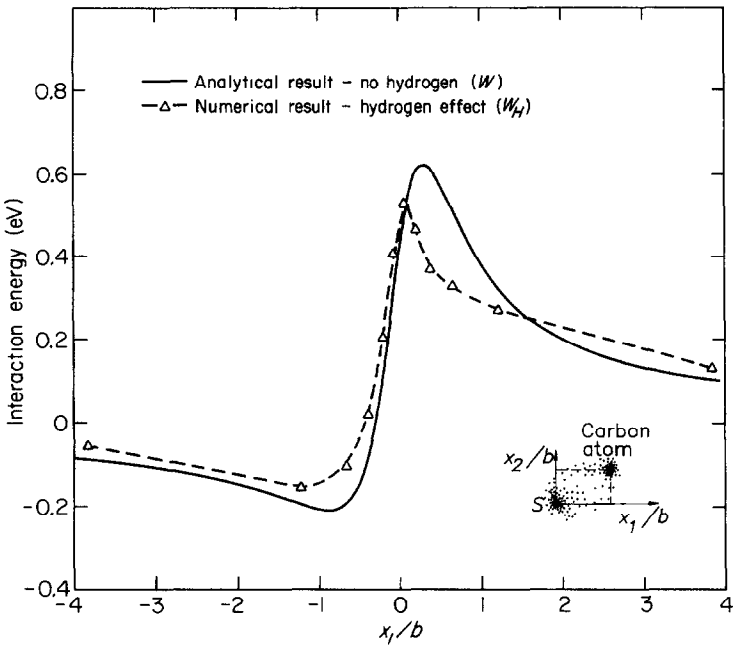

Fig. 21. Plot of the screw dislocation–carbon atom interaction energy measured in eV per slab of thickness a versus carbon atom position x_1/b, $x_2/b = -0.505$ relative to the dislocation for a carbon atom with a tetragonal axis [001]. The hydrogen effect was calculated at temperature 300 K and nominal hydrogen concentration of H/M = 0.1.

which generates an increased H/M value in the vicinity of the dislocation, the hydrogen atmosphere is completely determined by the second order interaction energy, equation (2). In the present calculations, the second order interaction energy is positive as the shear modulus increases with increasing H/M values and hence a hydrogen atmosphere will not occur around the screw dislocation, as is assumed. The case of a significant negative second order elastic interaction energy between solute hydrogen and the screw dislocation leading to a hydrogen atmosphere around the screw dislocation will be considered in a subsequent publication. As expected from the low hydrogen concentrations, the "global treatment" of Larche and Cahn (1985) results in a very small change in the magnitude of the elastic interaction energy between the screw dislocation and the C interstitial due to solute hydrogen. The changes are less than about 5% of the analytic result in the absence of hydrogen. This may be compared with the much larger changes calculated using the present methods, even in the present case where the increase of shear modulus with hydrogen minimizes the effects of hydrogen on the elastic interactions with the screw dislocation.

The interactions of screw dislocations with point defects having tetragonal symmetry are more complex than those which describe interactions with edge dislocations. One significant point is that the interaction can be asymmetric with respect to the direction of motion of the screw dislocation relative to the interstitial solute, e.g. for the system studied the interaction is asymmetric except for the C interstitial having the [100] tetragonal axis (Figs 19–21). The effects of hydrogen on the interactions of

the C interstitials with screw dislocations are correspondingly complex. For interactions with defects having the [100] tetragonal axis, the effect of hydrogen is to increase the interaction energy between the screw dislocation and the C solute (Fig. 19). For [010] and [001] tetragonal axis orientations, adding hydrogen to the system decreases the interaction energies in those regions where the C–screw dislocation interactions are repulsive and has little effect in the regions where there is an attractive interaction between the defects. The width of the repulsive interaction energy region is also significantly decreased by the addition of hydrogen.

All three C solute orientations are likely to be equally populated in the volume of a crystal far from dislocations. Close to the dislocation, the C solute having a [100] orientation of the tetragonal axis has the lowest energy, and since C reorientation can occur with only one defect jump, this orientation will be most highly populated. A moving screw dislocation is likely to experience interactions with all three C orientations with equal probability. The addition of hydrogen to the system will increase the population of C solutes having [100] orientations near the dislocation when the interactions allow reorientation of the C solute as H increases the magnitude of the attractive interaction between the screw dislocation and the [100] C solute. This should lead to a decrease in the mobility of the screw dislocations on adding H to the system containing C solutes at temperatures where they can reorient during the interactions. At lower temperatures, where reorientation of the C solutes is not possible, the effects of H on the carbon–screw dislocation interactions are more complex. The increased magnitude of the attractive interaction energy for [100] C solutes (which should decrease the dislocation mobility) is balanced against the decreased magnitude of the repulsive interactions for the [010] and [001] C solutes (which should increase the mobility). Both attractive and repulsive interactions need to be overcome during the motion of the dislocations. In the Fe–H system (Tabata and Birnbaum, 1984), screw dislocation mobility was observed to increase when hydrogen was added to the system. Detailed experimental measurements of these interactions have only been made in the Ni–C–H system (Sirois and Birnbaum, 1992). Since this is an FCC system and hence the C interstitial solutes have a cubic distortion field, the calculations of the present paper are not directly applicable.

4. CLOSURE

A method for calculating the effects of a mobile solute species, such as hydrogen, on the interaction between elastic centers has been developed. This method allows modeling of the lattice distortion induced by a single or a continuous distribution of interstitial atoms coupled with the distortion field of lattice defects such as dislocations. The method was applied using analytical and finite element methods to study the effects of hydrogen on the interaction between dislocations and between dislocations and solutes such as C interstitials. Included in the calculational method is the minimization of elastic energy of the system, thus allowing the hydrogen distribution to respond to the local stress field of the elastic centers. The mobile hydrogen solutes exhibit the phenomena of "elastic shielding" of the interactions between two elastic stress centers, i.e. the redistribution of the hydrogen solutes to

decrease the elastic energy of the system. In most cases this "elastic shielding" results in a decrease of the interaction energies and forces between the elastic centers.

Model calculations were carried out for the case where hydrogen increased the shear modulus of the system and in which the second order elastic interaction between the dislocations and hydrogen could be neglected. These calculations, by both finite element and analytical methods, of the hydrogen-induced "elastic shielding" of the interaction between two dislocations showed a decrease in the elastic force between the two dislocations which varied with the distance between the dislocations and with the hydrogen concentration. The effect was largest when the dislocations were separated by small distances and resulted from the lattice dilatation of the hydrogen solutes and their effect on the local elastic modulus of the matrix. For an H/M value of 0.01, the decrease of the force between two edge dislocations separated by three Burgers vectors was about 8% and this increased to about 21% for H/M = 0.1.

Calculations of the interactions between an edge dislocation and a C interstitial in a BCC solid were carried out using the method of Cochardt *et al.* (1955) and the effect of hydrogen on these interactions was studied. The carbon–edge dislocation interaction results from the dilatational stress around the C as well as from the deviatoric components. Significant decreases in the magnitude of the interaction energies between the edge dislocation and the C interstitial due to "elastic shielding" by hydrogen was observed when the C was less than two Burgers vectors below the slip plane. When the C was below the slip plane by greater than about two Burgers vectors, small increases in the magnitude of the interaction energies were observed. A decrease in the elastic interaction energy between the edge dislocation and the C interstitial was observed for all three orientations of the tetragonal axis of the C solute. These effects on the interaction energies were shown to be due predominantly to the H-induced local changes in the elastic moduli.

Hydrogen shielding effects were also studied for the interaction of C interstitials with screw dislocations in the BCC lattice. The carbon–screw dislocation interaction energy results from only the deviatoric components of the distortion field around the C. Hydrogen effects on the interaction energy in this case result from the local modulus changes due to the hydrogen atmosphere around the C interstitial. The effects of elastic shielding in this case are somewhat more complex than in the case of the edge dislocation interaction. The interaction energy of the screw dislocation with one of the C orientations is increased while those with the other two are decreased.

ACKNOWLEDGEMENT

This work was supported by the Department of Energy under grant DEFGO2-91ER45439.

REFERENCES

Bilby, B. A. (1950) On the interactions of dislocations and solute atoms. *Proc. Phys. Soc.* **A63,** 191–200.

Birnbaum, H. K. and Sofronis, P. (1994) Hydrogen-enhanced localized plasticity—a mechanism for hydrogen-related fracture. *Mater. Sci. Engng* **A176,** 191–202.

Bond, G. M., Robertson, I. M. and Birnbaum, H. K. (1987) The influence of hydrogen on deformation and fracture processes in high-strength aluminum alloys. *Acta Metall.* **35,** 2289–2296.

Bond, G. M., Robertson, I. M. and Birnbaum, H. K. (1988) Effects of hydrogen on deformation and fracture processes in high-purity aluminum. *Acta Metall.* **36,** 2193–2197.

Cochardt, A. W., Schoek, G. and Wiedersich, H. (1955) Interaction between dislocations and interstitial atoms in body-centered cubic metals. *Acta Metall.* **3,** 533–537.

Cottrell, A. H. (1948) Effects of solute atoms on the behaviour of dislocations. *Report of a Conference on Strength of Solids*, held at the H. H. Wills Physical Laboratory, University of Bristol, 7–9 July 1947, pp. 30–36. The Physical Society, London.

Cottrell, A. H. and Bilby, B. A. (1949) Dislocation theory of yielding and strain ageing of iron. *Proc. Phys. Soc.* **A62,** 49–62.

Cottrell, A. H. and Jawson, M. A. (1949) Distribution of solute atoms round a slow dislocation. *Proc. R. Soc.* **A199,** 104–114.

Eshelby, J. D. (1955) The elastic interaction of point defects. *Acta Metall.* **3,** 487–490.

Eshelby, J. D. (1956) The continuum theory of lattice defects. *Solid State Physics* (ed. F. Seitz and D. Turnbull), Vol. 3, pp. 79–144. Academic Press, New York.

Eshelby, J. D. (1957) The determination of the elastic field of an ellipsoidal inclusion and related problems. *Proc. R. Soc.* **A241,** 376–396.

Flannagan, T. B., Mason, N. B. and Birnbaum, H. K. (1981) The effect of stress on hydride precipitation. *Scripta Metall.* **15,** 109–112.

Fuentes-Samaniego, R., Gasca-Neri, R. and Hirth, J. P. (1984) Solute drag on moving edge dislocations. *Phil. Mag.* **A49,** 31–43.

Hirth, J. P. and Carnahan, B. (1978) Hydrogen adsorption at dislocations and cracks in Fe. *Acta Metall.* **26,** 1795–1803.

Hirth, J. P. and Lothe, J. (1982) *Theory of Dislocations*. John Wiley, New York.

Kirchheim, R. (1986) Interaction of hydrogen with external stress fields. *Acta Metall.* **34,** 37–42.

Larche, F. C. and Cahn, J. W. (1985) The interaction of composition and stress in crystalline solids. *Acta Metall.* **33,** 331–357.

Mazzolai, F. M. and Birnbaum, H. K. (1985a) Elastic constants and ultrasonic attenuation of the α–α' phase of the Nb–H(D) system. I: Results. *J. Phys. F: Met. Phys.* **15,** 507–523.

Mazzolai, F. M. and Birnbaum, H. K. (1985b) Elastic constants and ultrasonic attenuation of the α–α' phase of the Nb–H(D) system. II: Interpretation of results. *J. Phys. F: Met. Phys.* **15,** 525–542.

Peisl, H. (1978) Lattice strains due to hydrogen in metals. *Hydrogen in Metals I. Topics in Applied Physics* (ed. G. Alefeld and J. Volkl), Vol. 28, pp. 53–74. Springer, New York.

Robertson, I. M. and Birnbaum, H. K. (1986) An HVEM study of hydrogen effects on the deformation and fracture of nickel. *Acta Metall.* **34,** 353–366.

Rozenak, P., Robertson, I. M. and Birnbaum, H. K. (1990) HEVM studies of the effects of hydrogen on the deformation and fracture of AISI type 316 austenitic stainless steel. *Acta Metall.* **38,** 2031–2040.

Shih, D., Robertson, I. M. and Birnbaum, H. K. (1988) Hydrogen embrittlement of α titanium: *in situ* TEM studies. *Acta Metall.* **36,** 111–124.

Sirois, E. and Birnbaum, H. K. (1992) Effects of hydrogen and carbon on thermally activated deformation in nickel. *Acta Metall.* **40,** 1377–1385.

Sirois, E., Sofronis, P. and Birnbaum, H. K. (1992) Effects of hydrogen and carbon on thermally activated deformation in nickel. *Parkins Symposium on Fundamental Aspects of Stress Corrosion Cracking* (ed. S. M. Bruemmer, E. I. Meletis, R. H. Jones, W. W. Gerberich, F. P. Ford and R. W. Staehle), pp. 173–190. The Minerals, Metals & Materials Society.

Sofronis, P. and Birnbaum, H. K. (1993) Mechanics of hydrogen–dislocation–impurity interactions: part I–increasing shear modulus. TAM Report No. 729, UILU-ENG-93-6027, University of Illinois at Urbana-Champaign, Urbana, IL.

Stroh, A. N. (1957) A theory of the fracture of metals. *Adv. Phys.* **6,** 418–465.

Tabata, T. and Birnbaum, H. K. (1984) Direct observations of hydrogen enhanced crack propagation in iron. *Scripta Metall.* **18,** 231–236.

Zener, C. (1948) The micro-mechanism of fracture. *Fracturing of Metals*. American Society for Metals, Cleveland, OH.

APPENDIX A: HYDROGEN-INDUCED SHEAR STRESS ON THE DISLOCATION SLIP PLANE—NUMERICAL INTEGRATION OF (14)

Consider the integrand of (14) in the limit as $r \to 0$ along any radius such that $\pi < \phi < 2\pi$. This limit expresses the contribution to the shear stress τ_H of the hydrogen which resides at the core of the dislocation 2 (see Fig. 1). More specifically, it accounts for that part of the contribution that is found when the core is approached through the tensile region of the dislocation 2. On the tensile side of the core, the in-plane hydrostatic stress becomes infinite and the corresponding equilibrium hydrogen concentration is finite and equal to N_L. Therefore, the integrand of (14) is singular for a value of r, namely for $r = 0$, which is close to the lower limit of integration, r_2. When the core of the dislocation 2 is approached along a radial direction in the compressive region it can be easily shown that the concentration tends to zero at a faster rate than the radius, thus causing the integrand to be zero. At the core of the dislocation 1, that is at $r = l$, the hydrogen concentration is 0 on the side of the compressive region and N_L, on the side of the tensile region. Since r is equal to l, i.e. r is finite, the integrand of (14) at the core of dislocation 1 is finite as well. Again, the circular area of the core of the dislocation 1 was excluded from the integration.

The singularity at $r = 0$ is treated by changing the variable of integration, i.e. by setting $r = 1/x$. In terms of the new variable, x, (15) for the in-plane hydrostatic stress can be written as

$$\frac{\sigma_{11}^a + \sigma_{22}^a}{2} = -\frac{\mu}{2\pi(1-\nu)} x \left(b_2 \sin\phi + b_1 \frac{\sin\phi - xl\sin\omega}{1 + x^2 l^2 - 2xl\cos(\phi - \omega)} \right), \tag{A1}$$

whereas (14) becomes

$$\tau_H = -\frac{\mu}{2\pi(1-\nu)} \frac{V_H}{N_A} \int_0^{2\pi} \int_{1/R}^{1/r_2} C(x,\phi) \frac{\sin 2\phi}{x} \mathrm{d}x\, \mathrm{d}\phi. \tag{A2}$$

In the limit as $x \to 0$, (A1) gives zero in-plane hydrostatic stress which forces a finite equilibrium concentration equal to C_0, thereby causing the integrand of (A2) to be singular at $x = 0$. Expanding the concentration $C(x, \phi)$ in a Taylor series about $x = 0$ at constant ϕ one finds that

$$C(x,\phi) = C_0 + \left.\frac{\partial C(x,\phi)}{\partial x}\right|_{x=0} x + O(x^2), \tag{A3}$$

where it can be shown that the second term on the right hand side of (A3) is different from zero and finite. Therefore, (A2) may be recast into

$$\tau_H = -\frac{\mu}{2\pi(1-\nu)} \frac{V_H}{N_A} \int_0^{2\pi} \int_{1/R}^{1/r_2} \frac{C(x,\phi) - C_0}{x} \sin 2\phi \, \mathrm{d}x\, \mathrm{d}\phi, \tag{A4}$$

with the integrand now being finite at $x = 0$.

For a given outer cut-off radius, R, of the hydrogen atmosphere, the shear stress τ_H was evaluated numerically through (A4) by slicing the domain of integration in the ϕ direction into sectors of equal angle. In each sector the double integral of (A4) was calculated by using a 40 by 40 Gauss rule. The calculation was repeated by increasing the number of sectors until the value of the calculated shear stress τ_H was found to be independent of the number of sectors used.

APPENDIX B: INTERACTION ENERGY BETWEEN CONFIGURATION A (DISLOCATION AND ITS HYDROGEN ATMOSPHERE) AND CONFIGURATION B (CARBON ATOM AND ITS HYDROGEN ATMOSPHERE)

Excluding the area of the dislocation core region, S_{core}, one may write (33) as follows

$$\begin{aligned} W(\mathrm{D},\mathrm{C},\mathrm{H}) = {} & \frac{1}{2}\int_{S-S_{\text{core}}} (\sigma_{\mathrm{D}})_{ij}(\varepsilon_{\mathrm{D}})_{ij}\,\mathrm{d}S + \frac{1}{2}\int_{S-S_{\text{core}}} (\sigma_{\mathrm{D}})_{ij}(\varepsilon_{\mathrm{C}})_{ij}\,\mathrm{d}S + \frac{1}{2}\int_{S-S_{\text{core}}} (\sigma_{\mathrm{D}})_{ij}(\varepsilon_{\mathrm{H}})_{ij}\,\mathrm{d}S \\ & + \frac{1}{2}\int_{S-S_{\text{core}}} (\sigma_{\mathrm{C}})_{ij}(\varepsilon_{\mathrm{D}})_{ij}\,\mathrm{d}S + \frac{1}{2}\int_{S-S_{\text{core}}} (\sigma_{\mathrm{C}})_{ij}(\varepsilon_{\mathrm{C}})_{ij}\,\mathrm{d}S + \frac{1}{2}\int_{S-S_{\text{core}}} (\sigma_{\mathrm{C}})_{ij}(\varepsilon_{\mathrm{H}})_{ij}\,\mathrm{d}S \\ & + \frac{1}{2}\int_{S-S_{\text{core}}} (\sigma_{\mathrm{H}})_{ij}(\varepsilon_{\mathrm{D}})_{ij}\,\mathrm{d}S + \frac{1}{2}\int_{S-S_{\text{core}}} (\sigma_{\mathrm{H}})_{ij}(\varepsilon_{\mathrm{C}})_{ij}\,\mathrm{d}S + \frac{1}{2}\int_{S-S_{\text{core}}} (\sigma_{\mathrm{H}})_{ij}(\varepsilon_{\mathrm{H}})_{ij}\,\mathrm{d}S \\ & - \int_{s+s_{\text{core}}} (T_{\mathrm{D}})_i(u_{\mathrm{D}} + u^{(\mathrm{C})} + u^{(\mathrm{H})})_i\,\mathrm{d}s, \end{aligned} \tag{B1}$$

where s_{core} is the circular boundary of S_{core}. Symmetry $C_{ijkl} = C_{klij}$ of the elasticity tensor implies that

$$\begin{aligned} (\sigma_{\mathrm{C}})_{ij}(\varepsilon_{\mathrm{D}})_{ij} &= (\sigma_{\mathrm{D}})_{ij}(\varepsilon_{\mathrm{C}})_{ij}, \\ (\sigma_{\mathrm{H}})_{ij}(\varepsilon_{\mathrm{D}})_{ij} &= (\sigma_{\mathrm{D}})_{ij}(\varepsilon_{\mathrm{H}})_{ij}, \\ (\sigma_{\mathrm{C}})_{ij}(\varepsilon_{\mathrm{H}})_{ij} &= (\sigma_{\mathrm{H}})_{ij}(\varepsilon_{\mathrm{C}})_{ij}, \end{aligned} \tag{B2}$$

and by the principle of virtual work

$$\int_{S-S_{\text{core}}} (\sigma_{\mathrm{D}})_{ij}(\varepsilon_{\mathrm{D}})_{ij}\,\mathrm{d}S = \int_{S+S_{\text{core}}} (\mathrm{T}_{\mathrm{D}})_i(\mathrm{u}_{\mathrm{D}})_i\,\mathrm{d}s. \tag{B3}$$

Use of (B2), (B3) and

$$\begin{aligned} (\varepsilon_{\mathrm{C}})_{ij} &= (\varepsilon^{(\mathrm{C})})_{ij} - (\varepsilon^{\mathrm{C}})_{ij}, \\ (\varepsilon_{\mathrm{H}})_{ij} &= (\varepsilon^{(\mathrm{H})})_{ij} - (\varepsilon^{\mathrm{H}})_{ij} \end{aligned} \tag{B4}$$

in (B1) yields

$$\begin{aligned} W(\mathrm{D},\mathrm{C},\mathrm{H}) = {} & -\frac{1}{2}\int_{S-S_{\text{core}}} (\sigma_{\mathrm{D}})_{ij}(\varepsilon_{\mathrm{D}})_{ij}\,\mathrm{d}S + \int_{S-S_{\text{core}}} (\sigma_{\mathrm{D}})_{ij}(\varepsilon^{(\mathrm{C})} - \varepsilon^{\mathrm{C}})_{ij}\,\mathrm{d}S \\ & + \int_{S-S_{\text{core}}} (\sigma_{\mathrm{D}})_{ij}(\varepsilon^{(\mathrm{H})} - \varepsilon^{\mathrm{H}})_{ij}\,\mathrm{d}S + \int_{S-S_{\text{core}}} (\sigma_{\mathrm{H}})_{ij}(\varepsilon^{(\mathrm{C})} - \varepsilon^{\mathrm{C}})_{ij}\,\mathrm{d}S \\ & + \frac{1}{2}\int_{S-S_{\text{core}}} (\sigma_{\mathrm{C}})_{ij}(\varepsilon^{(\mathrm{C})} - \varepsilon^{\mathrm{C}})_{ij}\,\mathrm{d}S + \frac{1}{2}\int_{S-S_{\text{core}}} (\sigma_{\mathrm{H}})_{ij}(\varepsilon^{(\mathrm{H})} - \varepsilon^{\mathrm{H}})_{ij}\,\mathrm{d}S - \int_{s+s_{\text{core}}} (T_{\mathrm{D}})_i(u^{(\mathrm{C})} + u^{(\mathrm{H})})_i\,\mathrm{d}s. \end{aligned} \tag{B5}$$

By the principle of virtual work

$$\int_{S-S_{\text{core}}} (\sigma_{\mathrm{D}})_{ij}(\varepsilon^{(\mathrm{C})})_{ij}\,\mathrm{d}S = \int_{s+s_{\text{core}}} (T_{\mathrm{D}})_i(u^{(\mathrm{C})})_i\,\mathrm{d}s.$$

$$\int_{S-S_{core}} (\sigma_D)_{ij}(\varepsilon^{(H)})_{ij}\,dS = \int_{s+s_{core}} (T_D)_i(u^{(H)})_i\,ds, \tag{B6}$$

and substituting into (B5) one finds

$$\begin{aligned} W(D,C,H) = &-\frac{1}{2}\int_{S-S_{core}} (\sigma_D)_{ij}(\varepsilon_D)_{ij}\,dS - \int_{S-S_{core}} (\sigma_D)_{ij}(\varepsilon^C)_{ij}\,dS - \int_{S-S_{core}} (\sigma_D)_{ij}(\varepsilon^H)_{ij}\,dS \\ &+ \int_{S-S_{core}} (\sigma_H)_{ij}(\varepsilon^C)_{ij}\,dS - \int_{S-S_{core}} (\sigma_H)_{ij}(\varepsilon^C)_{ij}\,dS \\ &+ \frac{1}{2}\int_{S-S_{core}} (\sigma_C)_{ij}(\varepsilon^C)_{ij}\,dS - \frac{1}{2}\int_{S-S_{core}} (\sigma_C)_{ij}(\varepsilon^C)_{ij}\,dS \\ &+ \frac{1}{2}\int_{S-S_{core}} (\sigma_H)_{ij}(\varepsilon^{(H)})_{ij}\,dS - \frac{1}{2}\int_{S-S_{core}} (\sigma_H)_{ij}(\varepsilon^H)_{ij}\,dS. \end{aligned} \tag{B7}$$

As is explained in the formulation of the boundary value problem for the hydrogen stress field in Section 2.2, exclusion of the dislocation core area may be disregarded in the solution process of the carbon/hydrogen and carbon/no-hydrogen problems. Therefore, the domain of integration in all integrals of (B7), except the first, can be extended to include the core region S_{core} and thus its boundary S_{core} is eliminated. Then application of the principle of virtual work yields

$$\begin{aligned} &\int_S (\sigma_H)_{ij}(\varepsilon^{(C)})_{ij}\,dS = 0, \\ &\int_S (\sigma_C)_{ij}(\varepsilon^{(C)})_{ij}\,dS = 0, \\ &\int_S (\sigma_H)_{ij}(\varepsilon^{(H)})_{ij}\,dS = 0. \end{aligned} \tag{B8}$$

By substitution of (B8) into (B7) one finds

$$\begin{aligned} W(D,C,H) = &-\frac{1}{2}\int_{S-S_{core}} (\sigma_D)_{ij}(\varepsilon_D)_{ij}\,dS - \frac{1}{2}\int_S (\sigma_C)_{ij}(\varepsilon^C)_{ij}\,dS - \frac{1}{2}\int_S (\sigma_H)_{ij}(\varepsilon^H)_{ij}\,dS \\ &- \int_S (\sigma_D)_{ij}(\varepsilon^C)_{ij}\,dS - \int_S (\sigma_D)_{ij}(\varepsilon^H)_{ij}\,dS - \int_S (\sigma_H)_{ij}(\varepsilon^C)_{ij}\,dS. \end{aligned} \tag{B9}$$